Parameter sensitivity and identifiability for a biogeochemical model of hypoxia in the northern Gulf of Mexico☆

Marcus W. Beck*

USEPA National Health and Environmental Effects Research Laboratory, Gulf Ecology Division, 1 Sabine Island Drive, Gulf Breeze, FL 32561

John C. Lehrter

Dauphin Island Sea Lab, University of South Alabama, Dauphin Island, AL 36528

Lisa L. Lowe

Lockheed Martin IS & GS - Civil supporting the USEPA, Research Triangle Park, NC 27709

Abstract

Bio-geo-chemical models are useful tools in environmental sciences that can guide management and policy-making. Consequently, significant time and resources are spent developing these models in system-specific contexts. The optimization of model parameters to maximize precision, including transferability of these models to different systems, are fundamental concerns in the development and application of these tools. This study provides a context for understanding quantitative limitations of coupled hydrodynamic-ecological models by evaluating parameter sensitivity and identifability of a zero-dimensional (0-D) unit of a larger spatio-temporal model of hypoxia on the Louisiana continental shelf of Gulf of Mexico. The analysis provides a contrast of numeric and ecological certainty in parameter subsets using a systematic framework to infer larger trends in dissolved oxygen dynamics over time, having implications for understanding factors that contribute to environmental conditions that are detrimental to aquatic resources. In particular, we focus on issues of parameter identifiability using local sensitivity analyses to provide quantitative descriptions of numerical constraints on model precision. The sensitivity of state variables differed considerably with parameter changes, although most variables were responsive to changes in parameters that influenced planktonic growth rates. Variation in sensitivity had a direct correspondence with identifiability, such that only small subsets of the complete parameter set were characterized as having unique effects on the model output. As a result, we provide a set of parameter selection heuristics that can be used to identify parameters for model calibration that depend on relative sensitivity and ecological categories within the biogeochemical equations. Although these concerns have been expressed in the literature, they are rarely explicitly addressed or included in evaluations of water quality models. In addition to immediate implications for regional models, we provide a framework for describing the effects of parameter uncertainty and identifiability that can be applied to similar models to better inform environmental management.

Keywords: Coastal General Ecosystem Model (CGEM), Gulf of Mexico (GOM), Hypoxia, Identifiability, Sensitivity

1. Introduction

Hypoxia formation in bottom waters of coastal oceans occurs primarily from excess nutrient inputs from land-based sources (Justíc et al., 1987; Diaz and Rosenberg, 1995; Howarth et al., 1996). These events are

detrimental to aquatic organisms and have significant negative effects on economic resources derived from coastal ecosystems (Lipton and Hicks, 2003; Diaz and Rosenberg, 2011). An understanding of the biological, physical, and chemical processes that contribute to the growth of hypoxic areas is a critical concern for mitigating and preventing these negative impacts. Numerical ecosystem models are important tools that synthesize knowledge of ecosystem processes that contribute to hypoxia formation and for predicting the effects of proposed management activities or future scenarios (Scavia et al., 2004; Hagy and Murrell, 2007; Pauer et al., 2016). Unlike statistical models with more generic structures, simulation and process-based models include explicit descriptions of relevant processes that are constrained by empirical or observational data relevant to the system of interest (e.g. Omlin et al., 2001b; Eldridge and Roelke, 2010). These models are often coupled with hydrodynamic grids to provide spatially-explicit representations of patterns in three dimensions (Warner et al., 2005; Zhao et al., 2010; Ganju et al., 2016). Combined hydrodynamic and bio-geo-chemical models have been developed specifically to describe hypoxic conditions on the Louisiana continental shelf (LCS) in the northern Gulf of Mexico (GOM) (Fennel et al. 2013; Obenour et al. 2015; Pauer et al. 2016, Lehrter et al. in press). This area drains a significant portion of the continental United States through the Mississippi-Atchafalaya River Basin (MARB) and is the second largest hypoxic area in the world (Rabalais et al., 2002). Understanding processes that contribute to the frequency and duration of hypoxic events remains a critical research goal for the region, including the application of process-based models to characterize the current knowledge domain.

The development and application of a model represents a tradeoff between characteristics expected from the output or provided by the structural components. An idealized model is sufficiently generalizable across systems, provides results that are precise given the inputs, and includes components that are realistic descriptions of actual processes (Levins, 1966). Given that these characteristics cannot be simultaneously achieved, models are developed in partial dependence of reality and theoretical constructs, completely separate from both, or dependent on one or the other (Morrison and Morgan, 1999; Ganju et al., 2016). These challenges are analogous to the well-known bias-variance tradeoff in statistical models that balances the competing objectives of over- and under-fitting to an observed dataset. Process-based models are more commonly imbalanced between reality and theory, such that most are over-parameterized in an attempt to completely describe reality (Denman, 2003; Nossent and Bauwens, 2012; Petrucci and Bonhomme, 2014). Such over-parameterization, including use of many structural equations, can have serious implications for practical applications. Quantitative limitations of over-parameterization are analogous to degrees of freedom in standard statistical models as free parameters cannot be numerically estimated when constrained to an observed dataset (Kirchner, 2006). More importantly, over-parameterization can limit use across systems outside of the data domain and impose uncertainty in model predictions as realistic values for every variable may not be known or inaccurately applied from existing studies (Durand et al., 2002; Refsgaard et al., 2007; Wade et al., 2008). The application of process-based models to describe hypoxia dynamics has not been immune to these challenges and comprehensive approaches are needed to develop models that more carefully balance theory with reality (e.g., Snowling and Kramer, 2001).

Standard approaches for uncertainty analysis can be used to begin addressing model complexity issues. In the most general sense, uncertainty is evaluated relative to the effects of input conditions or the observed data used to calibrate a model, changes in parameter values, or variation in the structural components (i.e., observational, parameter, or structural uncertainty) (Beck, 1987). Evaluating parameter uncertainty is by far the most common and simplest means of evaluating model behavior. Although uncertainty analyses should be integrated throughout model development and application, parameters are more often evaluated post-hoc as a form of 'damage control' for further calibration. This approach is sometimes called inverse modelling where results from sensitivity analyses are used to guide calibration or fit of the developed model to observations (Soetaert and Petzoldt 2010, or confronting models with data, *sensu* Hilborn and Mangel 1997). Parameter sensitivity analysis combined with inverse modelling necessarily involves questions of parameter 'identifiability', where only a subset of parameters can be numerically constrained to the data as compared to the entire parameter set. Redundancies in parameter effects lead to unidentifiable models where optimal solutions may be empirically impossible (i.e., standard algorithms will not converge) or parameter values may be non-unique leading to the right answer for the wrong reason (Kirchner, 2006). An unidentifiable parameter or parameter set has effects on model output that can be undone or compensated for by alteration of other parameters. The concept of identifiable parameter subsets is not foreign to hypoxia or eutrophication models (Omlin et al., 2001a; Estrada and Diaz, 2010; Mateus and Franz, 2015), although there is a clear

need for greater integration of these concepts in model development (Fasham et al., 2006). Moreover, the inclusion of sensitivity and identifiability analyses in model tuning will require the adoption of conservative selection rules for parameters to calibrate given the number of unique combinations of parameter subsets for most models (e.g., Wagener et al., 2001a,b).

This study describes a parameter sensitivity analysis to evaluate identifiability of parameter subsets for a bio-geo-chemical model of hypoxia for the northern GOM. We evaluate a simple zero-dimensional (0-D) unit of a larger spatial-temporal model to explore relationships between multiple parameter sets and hypoxia dynamics on the LCS. Specifically, we provide empirical results to support the assumption that models are generally over-parameterized and only a finite and smaller subset of the larger parameter set can be optimized for a given research question or dataset. We provide explicit guidance for choosing such subsets of the parameter space given constraints on identifiability as directly related to sensitivity analyses. The objectives are to 1) identify the parameters that have the greatest influence on dissolved oxygen (O_2) using local sensitivity analysis, 2) quantify the identifiability of subsets of the total parameter space based on sensitivity, 3) and provide a set of heuristics for choosing parameters based on sensitivity, identifiability, and parameter categories. These principles were also applied to other state variables predicted by the model (ammonium, chlorophyll a (chl-a), irradiance, nitrate, particulate organic matter (POM), dissolved organic matter (DOM), and phosphorus). A final analysis evaluated identifiability relative to structural uncertainty to provide an example of extending these methods to more complex uncertainty assessments. Throughout, the optimum parameter set is defined as the chosen subset that represents the maximum number of identifiable parameters. 'Optimum' is both a qualitative description based on a research question or management goal and a quantitative objective based on numerical optimization criteria for fitting model output to a calibration dataset. These results can be used to refine existing models or guide application of models to novel contexts, such as downscaling or application to new environments. We conclude with a discussion of the implications for hypoxia formation in coastal regions, including management strategies for nutrient reduction and use of mechanistic models to inform decision-making.

2. Methods

2.1. Model description

Hypoxic events, defined as <2 mg L^{-1} of O_2 (< 64 mmol m^{-3}), occur seasonally in bottom waters in the northern GOM. The LCS receives high nutrient loads from the MARB that drains a significant portion of the continental United States. Nutrient-stimulated primary production in surface waters increases biological oxygen demand in bottom waters as sinking organic matter is decomposed (Bierman et al., 1994; Murrell et al., 2013). The hypoxic area averages 15,540 km^2 annually (1993-2015) with minimum concentrations observed from late spring to early fall. Seasonal variation is strongly related to carbon and nutrient export from the MARB (Lohrenz et al., 2008; Bianchi et al., 2010), whereas hydrologic variation, currents, and wind patterns can affect vertical salinity gradients that contribute to the formation of hypoxia (Wiseman et al., 1997; Paerl et al., 1998; Obenour et al., 2015).

This study evaluated the core unit of a recently developed hydrodynamic and ecological model that describes horizontal and vertical transport and mixing of state variables relevant for hypoxia in the northern GOM. The Coastal General Ecosystem Model (CGEM) includes elements from the Navy Coastal Ocean Model (Martin, 2000) for hydrodynamics on the LCS and a biogeochemical model with multiple plankton groups, water-column metabolism, and sediment diagenesis (Eldridge and Roelke, 2010). The hydrodynamic component of CGEM provides a spatially-explicit description of hypoxia using an orthogonal grid with an approximate horizontal resolution of 1.9 km^2 and twenty equally-spaced vertical sigma layers on the shelf (depth $\leq$ 100 m, with additional hybrid layers at deeper depths). The biogeochemical component includes equations for 36 state variables including six phytoplankton groups (with nitrogen and phosphorus quotas for each), two zooplankton groups, nitrate, ammonium, phosphate, dissolved inorganic carbon, oxygen, silica, and multiple variables for dissolved and particulate organic matter from different sources. Atmospheric and hydrological boundary conditions described in Hodur (1997) and Lehrter et al. (2013) are also included in CGEM.

The core unit of CGEM is FishTank, a 0-D model that implements the biogeochemical equations in Eldridge and Roelke (2010) and does not include any form of physical transport (i.e., advection, mixing, or surface flux) nor sediment diagenesis. Although FishTank was developed for specific application in CGEM,

it can easily be applied to other hydrodynamic grids. Accordingly, the sensitivity and identifiability analyses described below are informative for both the LCS gridded model as well as potential applications to different systems. The FishTank model provides estimates for the 36 state variables described above using a 0-D parcel that is uniformly mixed as a closed system. A set of initial conditions is provided on execution of the model that is based on observations of relevant variables obtained from research cruises in the northern GOM during April, June, and September of 2006 (Table 1 in Murrell et al., 2014).

Results from FishTank are based on time-dependent differential equations that describe energy flow between phytoplankton and zooplankton groups as affected by nutrient uptake rates, organic matter inputs and losses, inherent optical properties, and temperature (Penta et al. 2008; Eldridge and Roelke 2010, see appendix in Lehrter et al. in press). A total of 108 equations are estimated at each time step to return a value for each of the 36 state variables described by the model. In addition to the initial conditions, 251 parameter values for each of the equations are also supplied at model execution. These parameters define relationships among fixed effects in the equations and represent ecological properties described by the model that influence hypoxia formation. Values for each of the parameters were based on estimates from the literature, field or laboratory-based measurements, or expert knowledge in absence of the former. As such, a sensitivity analysis of parameter values is warranted given that, for example, literature or field-based estimates may not apply under all scenarios or expert knowledge is not completely certain (Refsgaard et al., 2007).

The sensitivity of O_2 to perturbations of all relevant parameters for the 108 equations was estimated using a five minute timestep of FishTank simulations from January 1st to December 31st, 2006. Irrelevant parameters were removed for several reasons; parameters were not relevant for the 0-D model (i.e., hydrodynamic parameters), were considered physical constants, or had no effect given initial conditions. Additionally, Fish-Tank includes six phytoplankton and two zooplankton groups to describe complexity in community structure and foodweb dynamics. However, structural equations for each group are identical such that chosen parameter values primarily control differences between the groups, e.g., large-bodied or small-bodied plankton, slow-growing or fast-growing plankton, etc. Initial analyses indicated that parameter sensitivity of dissolved oxygen was identical within the six phytoplankton and zooplankton groups. To remove obvious redundancies in the model, the sensitivity analyses were conducted using only one phytoplankton and one zooplankton group. The final parameter set that was evaluated included 51 parameters that were further grouped into one of six categories based on applicable biogeochemical components of the model: optics ($n = 4$ parameters), organic matter (12), phytoplankton (22), temperature (2), and zooplankton (11). A full description of the model parameters is available as an appendix in Lehrter et al. in press.

2.2. Local sensitivity analysis

The analysis focused on sensitivity of O_2 and other state variables (noted below) in the 0-D FishTank model to identify parameters that may affect spatial and temporal variation of hypoxia in the larger model. A local sensitivity analysis was performed by evaluating the change in O_2 following perturbation of each parameter from its original value. The analyses relied exclusively on concepts used in the FME package developed for the R statistical programming language (Soetaert and Petzoldt, 2010; RDCT (R Development Core Team), 2016). Parameters were individually perturbed by 50% of the original values and the model was executed to obtain an estimate of O_2 sensitivity. For each perturbation, a sensitivity value S was estimated for each time step i given a change for parameter j as:

$$S_{ij} = \frac{\partial y_i}{\partial \Theta_j} \cdot \frac{w_{\Theta_j}}{w_{y_i}} \tag{1}$$

where the estimate depended on the change in the predicted value for response variable y divided by the change in the parameter Θ_j multiplied by the quotient of scaling factors w for each. The scaling factors, w_{Θ_j} for the parameter Θ_j and w_{y_i} for response variable y_i, were set as the default value of the unperturbed parameter and the predicted value of y_i after perturbation (Soetaert and Petzoldt, 2010). The scaling ensures the estimates are unitless such that the relative magnitudes allow comparisons of model sensitivity to parameters and state variables that differ in scale. Sensitivity values for all j parameters were summarized across the time series from $i = 1$ to n as $L1$:

$$L1 = \sum |S_{ij}|/n \tag{2}$$

¹⁵⁸ The $L1$ value for each parameter was used as the primary measure of sensitivity for the state variables.
¹⁵⁹ All parameters for each of the six equation categories (optics, organic matter, phytoplankton, temperature,
¹⁶⁰ and zooplankton) that had non-zero $L1$ (suggesting sensitivity) were retained for identifiability analysis.

¹⁶¹ *2.3. Identifiability and selecting parameter subsets*

¹⁶² Identifiability of parameter subsets was estimated from the minimum eigenvector of the cross-product of
¹⁶³ a selected sensitivity matrix (Brun et al., 2001; Omlin et al., 2001a):

$$\gamma = \frac{1}{\sqrt{\min\left(\text{EV}[\hat{S}^\top \hat{S}]\right)}} \tag{3}$$

¹⁶⁴ where γ ranges from one to infinity for perfectly identifiable (orthogonal) or unidentifiable (perfectly collinear)
¹⁶⁵ results for parameters in a sensitivity matrix S. The sensitivity functions were supplied as a matrix $\hat{S}$ with
¹⁶⁶ rows i and columns j (eq. (1)) that described deviations of predicted O_2 from the default parameter values.
¹⁶⁷ Thus, γ can be estimated for any subset of parameter combinations using the change in model output for
¹⁶⁸ perturbations of individual parameters. Sensitivity matrices were first normalized by dividing by the square
¹⁶⁹ root of the summed residuals (Omlin et al., 2001a; Soetaert and Petzoldt, 2010).

¹⁷⁰ The collinearity index γ provides a measure of the linear dependence between sensitivity functions (i.e.,
¹⁷¹ S_i for j parameters) described above for subsets of parameters. Estimates of γ greater than 10-15 suggest
¹⁷² parameter sets are poorly identifiable (Brun et al., 2001; Omlin et al., 2001a), meaning parameter values
¹⁷³ that maximize precision on a calibration dataset are inestimable by conventional optimization algorithms
¹⁷⁴ given similar effects of the selected parameters on the estimated state variable. Greater sensitivity of a state
¹⁷⁵ variable to a subset of parameters does not always imply better identifiability if the effects of individual
¹⁷⁶ parameters are similar. An intuitive interpretation of γ is provided by Brun et al. (2001) such that a change
¹⁷⁷ in a state variable caused by a change in one parameter can be offset by the fraction $1 - 1/\gamma$ by the remaining
¹⁷⁸ parameters. That is, $\gamma = 10$ suggests the relative change in O_2 for an arbitrary parameter in the selected
¹⁷⁹ set can be compensated for by 90% with changes in the other parameters.

¹⁸⁰ Initial analyses suggested that considerably limited subsets of parameters were identifiable of the 51
¹⁸¹ evaluated for the FishTank model. Given this limitation, parameter selection must consider the competing
¹⁸² objectives of increased precision with parameter inclusion and reduced identifability as it relates to opti-
¹⁸³ mization. An additional challenge is the excessively high number of combinations of parameter sets, which
¹⁸⁴ complicates selection given sensitivity differences and desired ecological categories of each parameter (e.g.,
¹⁸⁵ practitioners may only be interested in optics parameters). For example, Fig. 1 provides a simple graphic
¹⁸⁶ of the unique number of combinations that are possible for different subsets of 'complete' parameter sets
¹⁸⁷ of different sizes (i.e., based on n choose k combinations equal to $n!/(k!(n-k)!)$). The number of unique
¹⁸⁸ combinations increases with the total parameters in the set and is also maximized for moderate selections
¹⁸⁹ (e.g., selecting half the total). For example, over 10^{14} combinations are possible by selecting 25 parameters
¹⁹⁰ from a set of 50. Accordingly, parameter selection is complicated by differing sensitivity, identifiability limits
¹⁹¹ for parameter subsets, and the difficulty of choosing from many combinations.

¹⁹² A set of heuristics was developed that address the tradeoff in model complexity and identifiability given
¹⁹³ the challenges described above (see also Wagener et al., 2001a). These rulesets were developed with the
¹⁹⁴ assumption that parameters will be selected with preference for those with high sensitivity and identifability
¹⁹⁵ based on $\gamma < 15$ as an acceptable threshold for subsets (e.g., 93% accountability). Selection heurestics also
¹⁹⁶ recognized that parameter categories (i.e., optics, organic matter, phytoplankton, temperature, zooplankton)
¹⁹⁷ may have unequal preferences by model users given questions of interest. In all selection scenarios, parameters
¹⁹⁸ were selected by decreasing sensitivity starting with the most sensitive until identifiability did not exceed
¹⁹⁹ $\gamma = 15$ where selections were 1) blocked within parameter category, 2) independent of parameter category,
²⁰⁰ 3) or considering all categories equally. The selection rules produced seven subsets of parameters that could
²⁰¹ further be used to optimize model calibration.

²⁰² *2.4. Observational and structural uncertainty*

²⁰³ In addition to parameter uncertainty, the effects of observational and structural uncertainty on the
²⁰⁴ sensitivity analyses were evaluated by changing the initial conditions and structural components, respectively,

from the default model setup. First, observational uncertainty (i.e., effects of observed data on model output) was evaluated by varying the initial conditions that were based on observational data from research cruises in the northern GOM (Murrell et al., 2014). Uncertainty in these data translates directly to uncertainty that can influence results of the sensitivity analysis. For example, the sensitivity of O_2 to variation in the half-saturation constants for phytoplankton (the concentration supporting half the maximum uptake rate of nutrients) will vary given the initial nutrient concentrations (Eppley et al., 1969). Further, changes in the ratio between nitrogen and phosphorus could affect sensitivity depending on the limiting nutrient. Parameter sensitivity was re-evaluated by varying all initial conditions that were non-zero by different seasonal means based on averages of water quality data across stations and years. April and September seasonal averages of the observed data were used to evaluate the effects of conditions that were typical of spring and late summer on the LCS (Table 1).

The effects of model structure on parameter sensitivity (i.e., structural uncertainty) were evaluated by changing specific components of the model. The FishTank model includes several ecosystem processes or characteristics that can be included based on expected conditions, available data, or desired complexity. These 'switches' are conceptually different from model parameters as they allow the inclusion or exclusion of explicit equations or processes. Switches in FishTank include different structural equations for the vertical attenuation of light through the water column (inherent or apparent optical properties, Penta et al. 2009; Eldridge and Roelke 2010) and chlorophyll to carbon ratio models (fixed or dynamic given light and nutrients, Cloern et al. 1995). Several switches also affect phytoplankton growth including different models for specific growth and effects of temperature, light dependence, nutrient uptake, and internal cell quotas (Lehrter et al. in press, references therein).

Parameter sensitivity was evaluated by comparing the results from the default model setup to a more complex setup with alternative switches (Table 2). The scenarios used switches for different equations to represent structural relationships of phytoplankton growth patterns with temperature, nutrient uptake, cell quotas, chl-a to carbon ratios, photosynthesis dynamics, and specific growth limits. The default scenario modelled phytoplankton growth with temperature as a sigmoidal function (Eldridge and Roelke, 2010), nutrient uptake as Michaelis-Menten kinetics (Dugdale and Goering, 1967), internal cell quotas following Droop (1973), chl-a to carbon ratios as a simple regression (Murrell et al., 2014), light-dependence of photosynthesis with photoinhibition (Platt et al., 1980), and a specific growth rate following Leibig's law of the minimum. Conversely, the complex scenario used switches that modelled relationships between phytoplankton growth with temperature using the Arrhenius model (Geider et al., 1997), nutrient uptake as proposed by Lehman et al. (1975) and modified in Geider et al. (1998), internal cell quotas following Flynn (2003), chl-a to carbon ratios following Cloern et al. (1995), light-dependence of photosynthesis that is nutrient dependent (Flynn, 2003), and a specific growth rate that is nutrient dependent. Complete details of model switches are provided as supplementary material to Lehrter et al. in press.

2.5. Extension to other state variables

The above analyses were repeated for additional state variables estimated by FishTank to provide further descriptions of ecological dynamics that are relevant for hypoxia. In addition to O_2, other state variables that were evaluated were ammonium, chl-a, irradiance, nitrate, POM, DOM, and phosphorus. Particulate and dissolved organic matter were estimated as the summation of the respective outputs for organic matter from phytoplankon ($OM1\_A$, $OM2\_A$) and fecal pellets from zooplankton ($OM1\_Z$, $OM2\_Z$, see Lehrter et al. in press).

3. Results

3.1. Local sensitivity analysis

Local sensitivity analyses showed that O_2 was sensitive to perturbations in 38 of the 51 (75% of total) parameters that were evaluated in FishTank (default panel Fig. 2, Table 3). Within each parameter category, O_2 was sensitive to three parameters for optics (75% of all optic parameters), eight for organic matter (67%), 16 for phytoplankton (73%), one for temperature (50%), and 10 for zooplankton (91%). Although O_2 had the greatest sensitivity to parameters in the zooplankton category (as percentage of total), the relative effects varied. Among all parameters, sensitivity values ranged from $L1 = 8.34 \times 10^{-8}$ for $QminP$ (phytoplankton)

to 0.05 for *umax* (phytoplankton), whereas average sensitivity among all parameters was $L1 = 9.2 \times 10^{-3}$. Within categories (excluding temperature with one sensitive parameter), sensitivity ranged from 4.39×10^{-5} (*astarOMA*) to 7.51×10^{-4} (*astar490*) for optics, 4.17×10^{-4} (*KNH4*) to 6.15×10^{-3} (*KG1*) for organic matter, 8.34×10^{-8} (*QminP*) to 0.05 (*umax*) for phytoplankton, and 3.69×10^{-5} (*ZQp*) to 0.05 (*ZKa*) for zooplankton (Table 3). Average sensitivity values in each category were $L1 = 2.81 \times 10^{-4}$ for optics, 2.17×10^{-3} for organic matter, 0.02 for temperature, 0.01 for phytoplankton, and 0.01 for zooplankton.

Local sensitivity analyses for the additional state variables (ammonium, chl-*a*, irradiance, nitrate, POM, DOM, and phosphorus) had similar results as O_2 with some exceptions (Fig. 2 and Tables S1 to S7). All variables were sensitive to the same parameters as O_2 (38 of 51 evaluated), although average sensitivity differed between variables. Average $L1$ ranged from 0.02 for irradiance (Table S3) to 0.71 for DOM (Table S6). All average sensitivity values for the state variables were higher than the average for O_2 ($L1 = 9.2 \times 10^{-3}$). For each variable, $L1$ ranged from 2.24×10^{-6} (*QminP*) to 8.49 (*mA*) for ammonium (Table S1), 1.38×10^{-6} (*QminP*) to 13.94 (*mA*) for chl-*a* (Table S2), 1.92×10^{-7} (*QminP*) to 0.13 (*ZKa*) for irradiance (Table S3), 6.67×10^{-7} (*QminP*) to 8.49 (*umax*) for nitrate (Table S4), 6.41×10^{-5} (*KNH4*) to 7.22 (*mA*) for POM (Table S5), 7.41×10^{-5} (*KNH4*) to 14.25 (*mA*) for DOM (Table S6), and 8.21×10^{-7} (*QminP*) to 1.47 (*ZKa*) for phosphate (Table S7). For the parameter categories, ammonium was most sensitive to phytoplankton parameters (average $L1 = 0.8$ across all parameters in the category), chl-*a* to phytoplankton ($L1 = 1.14$), irradiance to zooplankton ($L1 = 0.03$), nitrate to zooplankton ($L1 = 1.06$), POM to temperature ($L1 = 0.86$), DOM to temperature ($L1 = 1.48$), and phosphate to zooplankton ($L1 = 0.31$). Finally, average sensitivity between parameter categories independent of the state variables ranged from 8.38×10^{-3} for optics (average $L1$ across all variables) to 0.62 for phytoplankton.

3.2. Subset identifiability

The identifiability analyses suggested that many parameter subsets exceeded the thresholds of $\gamma = 10, 15$, providing further justification for using selection heuristics for parameter optimization. Results for O_2 are provided first to demonstrate general concepts for the identifiability analyses, followed by an extension to the remaining state variables. Parameter identifiability for O_2 decreased (increasing γ) at different rates with increasing size of parameter subsets depending on the parameter category or the number of top parameters that were selected (Fig. 3). By category, identifiability was lowest for all combinations of parameter subsets in the phytoplankton (60% of subsets less than $\gamma = 15$, 43% less than $\gamma = 10$) and zooplankton categories (53.1% less than $\gamma = 15$, 40% less than $\gamma = 10$), whereas all combinations were identifiable for optics (100% less than $\gamma = 15, 10$) and a majority identifiable for organic matter (91.9% less than $\gamma = 15$, 76.5% less than $\gamma = 10$). Identifiability for parameters in the temperature category was not evaluated because O_2 was sensitive to only one parameter (i.e., $\gamma = 1$). Parameter combinations for choosing from the top, top two, top three, and top four parameters in each category together had decreasing identifability with the increasing size of the selection pool (e.g., top one versus top four parameters, Fig. 3). The percentage of parameter subsets that were below the acceptable thresholds for identifability was 100% less than $\gamma = 15, 10$ for the top parameter in each category, 90.6% and 80.7% for the top two, 80.7% and 70.9% for the top three, and 55.8% and 45.7% for the top four. Results for the remaining state variables had similar patterns in identifiability with increasing size of parameter subsets and selection categories, although differences in identifiabiltiy between state variables was observed (Fig. 4). Most notably, nitrate was consistently the least identifiable variable (highest overall γ), whereas O_2 was most identifiable.

An alternative view of the results in Fig. 3 can be used to demonstrate the effects of parameter selection criteria and number of parameters in the selection pool on identifiability. Fig. 5 shows the percentage of identifiable parameter sets for O_2 using the same selection criteria in Fig. 3, i.e., selection of parameters only within parameter categories and selection of the top sensitive parameters regardless of category. Fig. 5 is similar to Fig. 3, with the added effect of a chosen γ threshold on identifiability. Previous studies have provided only general rules for γ thresholds (Brun et al., 2001; Omlin et al., 2001a), such that exact values for which parameter sets are inestimable likely vary between models and optimization methods. As such, multiple values are shown in Fig. 5 given that actual thresholds could vary in practice. In general, identifiability decreased with the addition of parameters, although the rate of decrease depended on the selected threshold for γ. More conservative values for γ (e.g., $\gamma = 5$) were more sensitive to the number of parameters in a subset, that is, identifiability decreased more quickly with the addition of parameters at lower γ thresholds

as compared to higher γ. Notable differences in identifiability were also observed by parameter selection criteria (within categories or top parameters only), which further supports results in Figs. 3 and 4.

An evaluation of the effects of individual parameters on γ suggested that some parameters had disproportionate effects on identifiability. Based on $\gamma = 15$, Fig. 3 suggests that most parameter sets for organic matter were identifiable, regardless of how many parameters were selected (i.e., two through eight). However, some subsets were not identifiable such that identification of one or more redundant parameters that are inflating γ values could provide useful information. Fig. 6 shows an alternative view of identifiability of O_2 with exclusion and inclusion of individual parameters in different sets for the organic matter category. As before, collinearity increases with more parameters in a subset, although the increase varies depending on which parameter was included or excluded from the set. For example, inclusion of *KNO3* in a parameter set almost always inflated γ. All parameter subsets that did not include *KNO3* were well below $\gamma = 15$, suggesting that removal of this parameter improves identifiability. Interestingly, the inclusion of some parameters caused a reduction in γ, which contradicts the general rule that more parameters caused reduced identifiablity. For example, parameter sets that included *KGcdom* generally had lower γ values relative to those that excluded the parameter.

3.3. Parameter selection

The above results demonstrated that state variables differed in the magnitudes of sensitivity for each parameter and the number of identifiable subsets, where the latter varied by γ thresholds and parameter selection criteria. Results for each of the three selection heuristics (blocked by parameter category, independent of category, all categories equally) applied to each state variable differed in the number of selected parameters and distribution of parameters within each category (Tables 4 to 6). In general, a correspondence was observed between the number of parameters that were selected given the threhold of $\gamma = 15$ and relative identifiability between the state variables. As noted above, nitrate was the least identifiable variable (Fig. 4), whereas other variables (e.g., O_2, irradiance) were more identifiable. The constraints on identifiability between variables were demonstrated with the selection heuristics. For example, heuristics for nitrate typically selected only one or two parameters that met the criteria as compared to more identifiable variables that included several parameters. Overall, the first selection heuristic demonstrated that the number of parameters chosen by parameter category differed independently of the state variables (Table 4). The number of selected parameters averaged across state variables in decreasing order was 4.25 parameters from the phytoplankton category, 3.5 from organic matter, 2.75 from optics, and 2.38 from zooplankton. The second and third selection heuristics (Tables 5 and 6) were similar, although more parameters were generally selected for the third heuristic given equal importance between categories.

Fig. 7 demonstrates parameter selection for all state variables following the second heuristic where parameters were chosen by decreasing sensitivity independent of parameter categories (exact values are shown in Table 5). The y-axis shows the relative identifiability with the addition of parameters from one to many on the x-axis (from left to right). The second to last parameter for each variable is the last parameter selected within the potential threshold of $\gamma = 15$. Interestingly, the last parameter shown for most of the state variables caused a relatively large increase in γ that was disproportionate to the combined identifiability of the preceding parameter set. For most variables, the phytoplankton edibility vector for zooplankton (*ediblevector(Z1)*) caused a dramatic increase in γ with inclusion in the parameter set. In addition to demonstrating the approach for selection with the second heuristic, Fig. 7 provides an alternative method of identifying parameters that are disproportionately redundant within a given parameter set (i.e., large contribution to γ). This infomation is useful if additional parameter selection rules are developed independently of those proposed herein.

3.4. Observational and structural uncertainty

Both the relative $L1$ estimates and number of parameters that affected state variables were sensitive to variation in the initial conditions (observation effects) and structural changes in the model. Visual comparison of sensitivity values ($L1$) for the default model setup showed that all state variables were sensitive to *vmaxSi* after changing the initial conditions to April or September conditions (Fig. 2). State variables were also sensitive to *Ksi* for only the September conditions. Changing the model structure from the default (simple) to the complex setup showed state variables were also sensitive to *KQn* and *Tref(nospA+nospZ)$_{z1}$*. Changes in the sensitivity of individual parameters were also observed, most notably as a disproportionate increase in

L1 for ammonium, chl-*a*, POM, and DOM to *mA* and *Tref(nospA+nospZ)*$_{p1}$ using the complex model setup. Summaries by parameter categories of the effects of initial conditions and structural changes are shown in Table 7 and Fig. 8. Changes in average sensitivity using April and September initial conditions showed most variables were less sensitive to parameters in the optics, temperature, and zooplankton categories, whereas increased sensitivity was generally observed for parameters in the organic matter and phytoplankton categories. Some exceptions were observed, such as a decrease in nitrogen sensitivity to phytoplankton parameters (Table 7). Effects of structural complexity were most apparent as an increase in sensitivity of state variables to phytoplankton and temperature parameters, as noted for the individual variables in Fig. 2.

4. Discussion

4.1. Implications of sensitivity and identifiability analyses

Common goals in the application of biogeochemical models of ecosystem processes are to 1) accurately describe the system by matching predictions with observed data (Reckhow et al., 1990), and 2) provide a means of forecasting ecosystem condition with hypothesized management or environmental scenarios (Clark et al., 2001). Although these objectives are the focus of most applications, the structural components of process-based models should secondarily provide inference into which ecosystem processes and functions are driving observed changes. This latter objective represents a more generic scientific purpose of biogeochemical models that extends beyond the applied benefits of describing and predicting change in a particular system. Modelers often hope to identify universal principles that govern dynamics across systems and the constraint of model parameters to observations provides a means of supporting or refuting hypotheses (Kirchner, 2006). Extension of these principles to test the effects of structural changes and observation uncertainty on model predictions provides further information to support validation of model components. This study provided a simple approach to use the effects of parameter perturbations on model state variables to characterize identifiable parameter subsets that vary by parameter selection criteria. By doing so, we demonstrated that small parameter subsets relative to all sensitive parameters were within the identifiabilty thresholds described in the literature. The identifiable parameter subsets varied considerably between state variables and the method for parameter selection. We further demonstrated that changes in the model structure and variation in the initial conditions had an effect on sensitivity which has direct implications for identifiability. In general, these results provide justification for the use of explicit parameter selection heuristics that practitioners should adopt to facilitate model calibration.

Although the results were specific to individual variables, some generalities about hypoxia dynamics can be inferred from the sensitivity analyses. State variables were most sensitive to parameters in the phytoplankton and zooplankton categories, particularly the maximum growth rates (*umax* for phytoplankton, *Zumax* for zooplankton), mortality coefficient for phytoplankton (*mA*), and the zooplankton half saturation coefficent for grazing (*ZKa*). An increase in the growth rate of primary producers has the potential to increase oxygen concentration through photosynthetic processes, although increased production of organic matter is balanced with respiration and bacterial decomposition that reduce O_2 in the water column. Similarly, increases in zooplankton abundance with increased growth rates causes a reduction in phytoplankton biomass through grazing, which is expected to further deplete pools of organic matter. Most variables were also sensitive to variation in the half-saturation grazing coefficient which moderates the concentration of nutrients that support half the maximum grazing rate. Although the tradeoff between abundance, grazing, and decomposition is complex, the sensitivity of model state variables to parameters that directly control the abundance of primary producers is in agreement with empirical observations of factors that influence hypoxia dynamics on the LCS (Fahnenstiel et al., 1995; Roelke, 2000; Eldridge and Roelke, 2010). The sensitivity of the model output to variation in other parameters that relate to physical and chemical properties of the system was of secondary importance to biological relationships. That is, state variables were sensitive to changes in light and temperature parameters, although to a lesser extent than phytoplankton and zooplankton parameters. As such, the differing sensitivities of state variables to parameters in each of the categories was not unexpected given general ecological relationships that are well understood and described by the model.

The overwhelming conclusion from the identifiability analyses is that only limited subsets of parameters were identifiable within the constraints of local sensitivity analyses. Although we have not attempted actual model calibration (see recommendations below), these results support previous studies that have suggested

similarly small subsets of parameters can be identified using traditional calibration schemes (e.g., Wheater et al., 1986; Ye et al., 1997; Omlin et al., 2001a). In addition to CGEM, these conclusions have relevance for many biogeochemical models that include numerous parameters and structural equations to characterize processes in the model domain. A general conclusion is that perhaps a trend towards less complex models could be beneficial given that only a small subset of parameters is identifiable and that ecosystem processes may in fact be sufficiently characterized with few parameters (Ye et al., 1997). Conversely, others have argued that model complexity is not in itself a disadvantage when parsimony is not the sole arbitrator of model structure (Reichert and Omlin, 1997). Over-parameterization can be useful if processes have importance that were not evaluated during model identification. Single objective functions that maximize model precision with identifiable parameters may also provide an incomplete characterization of model worth, which has prompted the development of probability-based models of hypoxia that explicitly include uncertainty in model components (e.g. Obenour et al., 2015). Our results demonstrated that approximately 75% of the evaluated parameters had an effect on the eight state variables, whereas CGEM includes a total of 36 variables and multiple plankton groups, not all of which have immediate concern for understanding hypoxia. The redundancies identified with the sensitivity analyses are only problematic if the primary interest is, for example, O_2 dynamics. Moreover, the proposed selection heuristics provide flexibility for choosing different parameters with the assumption that those chosen depend on the research or management question.

Results from the identifiability analyses provided additional insight into the interactions of parameters in large biogeochemical models. First, identifiability of parameter subsets was not related to the sensitivity of individual variables. As noted above, an identifiable parameter is one that has a unique effect on model predictions that cannot be compensated for or undone by changing other parameters. The magnitude of the effect of a parameter has no bearing on identifiability, which further complicates the selection of parameters for calibration. Although identifiability is the primary limiting factor in choosing a set, the relative sensitivities are more important for the decision to include or exclude individual parameters. Our analysis addressed this challenge by presenting multiple selection criteria for identifiable parameter sets that prioritized the most sensitive parameters during the selection process. Similarly, identifability was not always related to the number of parameters in a set. Although the overwhelming trend was decreasing identifiability with more parameters, the unique effects of including an individual parameter with an existing set often reduced the γ estimate. For example, Fig. 6 shows that including *KGcdom*, *KO2*, or *nitmax* in parameter sets more often reduced γ relative to sets that excluded the parameters. Conversely, Fig. 7 showed that the inclusion of a specific parameters often caused a disproportionate increase in γ (e.g., *ediblevector(Z1)*). These examples demonstrate the complex interactions of parameter changes on variable response, highlighting the need to consider the combined and individual effects of parameters on identifiability. The selection criteria proposed in our above analyses can facilitate parameter selection and also provide diagnostic tools to identify parameters with disproportionate effects on γ.

4.2. Recommendations and conclusions

An evaluation of parameter uncertainty and identifiability of relevant parameter sets is a preliminary and simplistic approach to improving model predictions. In general, uncertainty analyses that lead to improved models are ultimately expected to increase our understanding of properties defining ecological relationships. The extension of simple parameter sensitivity analyses to the generalization of ecosystem properties requires additional analysis and potential model refinement, at the core of which is the balance between generality and precision. We emphasize that the utility of a specific model depends on the question and objective for application to a specific system. For the above analysis, the FishTank model, as part of the larger CGEM application, was evaluated in the context of hypoxia effects on ecosystem condition and function. At the core of the simple model is a set of biogeochemical equations that characterize the system in relation to planktonic groups, nutrient requirements, and water-column metabolism. Our results have shown that relatively small subsets of parameters are identifiable given the complexity of the model, and as a result, we have provided a general approach to select parameter subsets depending on the ecological context (i.e., selection by parameter category, selection for specific state variables). Thus, the results described above have relevance for further model refinement with the specific goal of better understanding ecological dynamics that moderate hypoxia on the northern GOM. However, the general principles of sensitivity and parameter identifiability have broad applicability beyond this context and we argue that such methods should be more universally applied as an initial approach to quantify numerical constraints of biogeochemical models.

Specific approaches can be used to improve and build on the results presented herein, in addition to the more general considerations noted above. An evaluation of model precision following calibration with relevant parameter subsets could provide additional information that supports results from the sensitivity analyses. For simplicity, our analysis did not calibrate model parameters and an explicit assumption was that parameter subsets with γ below 10 or 15 were identifiable. To our knowledge, this threshold has not been rigorously evaluated and it is likely to vary between parameter subsets and the chosen calibration method. Variation in parameter estimates given the calibration method and different identifiability thresholds could affect the interpration of model output. Further, the extent to which results for the 0-D model extrapolate to the larger three-dimensional model should be evaluated. Although the above analyses were facilitated using the 0-D model (i.e, quick execution times, ease of changing model parameters), lack of physical transport or spatial components potentially limits extrapolation of the results. Uncertainy in parameter estimates at lower dimensions could be magnified as errors propagate to larger scales or site-specific observations for model calibration are not appropriate across a hydrodynamic grid (Harvey, 2000; Lehrter and Cebrian, 2010). The effects of structural or observational uncertainty should also be evaluated in the context of the larger model. Our simple approach to examine changes in the initial conditions and switches used in the model showed that sensitivity estimates of individual parameters differed relative to the original model configuration, having further implications for characterizing identifiability.

Beck, M. B., 1987. Water quality modeling: A review of the analysis of uncertainty. Water Resources Research 23 (8), 1393–1442.

Bianchi, T. S., DiMarco, S. F., Jr, J. H. C., Hetland, R. D., Chapman, P., Day, J. W., Allison, M. A., 2010. The science of hypoxia in the Northern Gulf of Mexico: a review. Science of the Total Environment 408 (7), 1471–1484.

Bierman, V. J., Hinz, S. C., Zhu, D. W., Wiseman, W. J., Rabalais, N. N., Turner, R. E., 1994. A preliminary mass-balance model of primary productivity and dissolved oxygen in the Mississippi River plume/ inner Gulf shelf region. Estuaries 17 (4), 886–899.

Brun, R., Reichert, P., Künsch, H. R., 2001. Practical identifiability analysis of large environmental simulation models. Water Resources Research 37 (4), 1015–1030.

Clark, J. S., Carpenter, S. R., Barber, M., Collins, S., Dobson, A., Foley, J. A., Lodge, D. M., Pascual, M., Pielke, R., Pizer, W., Pringle, C., Reid, W. V., Rose, K. A., Sala, O., Schlesinger, W. H., Wall, D. H., Wear, D., 2001. Ecological forecasts: an emerging imperative. Science 293 (5530), 657–660.

Cloern, J. E., Grenz, C., Vidergar-Lucas, L., 1995. An empirical model of the phytoplankton:carbon ratio - the conversion factor between productivity and growth rate. Limnology and Oceanography 40 (7), 1313–1321.

Denman, K. L., 2003. Modelling planktonic ecosystems: parameterizing complexity. Progress in Oceanography 57 (3-4), 429–452.

Diaz, R. J., Rosenberg, R., 1995. Marine benthic hypoxia: A review of its ecological effects and the behavioural responses of benthic macrofauna. Oceanography and Marine Biology 33, 245–303.

Diaz, R. J., Rosenberg, R., 2011. Introduction to environmental and economic consequences of hypoxia. International Journal of Water Resources Development 27 (1), 71–82.

Droop, M. R., 1973. Some thoughts on nutrient limitation in algae. Journal of Phycology 9, 264–272.

Dugdale, R. C., Goering, J. J., 1967. Uptake of new and regenerated nitrogen in primary productivity. Limnology and Oceanography 12, 196–206.

Durand, P., Gascuel-Odoux, C., Cordier, M. O., 2002. Parameterisation of hydrological models: a review and lessons learned from studies of an agricultural catchment (Naisin, France. Agronomie 22 (2), 217–228.

Eldridge, P. M., Roelke, D. L., 2010. Origins and scales of hypoxia on the Louisiana shelf: importance of seasonal plankton dynamics and river nutrients and discharge. Ecological Modelling 221 (7), 1028–1042.

Eppley, R. W., Rogers, J. N., McCarthy, J., 1969. Half-saturation constants for uptake of nitrate and ammonium by marine phytoplankton. Limnology and Oceanography 14 (6), 912–920.

Estrada, V., Diaz, M., 2010. Global sensitivity analysis in the development of first principle-based eutrophication models. Environmental Modelling and Software 25, 1539–1551.

Fahnenstiel, G. L., McCormick, M. J., Lang, G. A., Redalje, D. G., Lohrenz, S. E., Markowitz, M., Wagoner, B., Carrick, H. J., 1995. Taxon-specific growth and loss rates for dominant phytoplankton populations from the northern Gulf of Mexico. Marine Ecology Progress Series 117 (1-3), 229–239.

Fasham, M. J. R., Flynn, K. J., Pondaven, P., Anderson, T. R., Boyd, P. W., 2006. Development of a robust marine ecosystem model to predict the role of iron in biogeochemical cycles: A comparison of results for iron-replete and iron-limited areas, and the SOIREE iron-enrichment experiment. Deep-Sea Research I 53, 333–366.

Fennel, K., Hu, J., Laurent, A., Marta-Almeida, M., Hetland, R., 2013. Sensitivity of hypoxia predictions for the northern Gulf of Mexico to sediment oxygen consumption and model nesting. Journal of Geophysical Research: Oceans 118 (2), 990–1002.

Flynn, K. J., 2003. Modelling multi-nutrient interactions in phytoplankton; balancing simplicity and realism. Progress in Oceanography 56 (2), 249–279.

Ganju, N. K., Brush, M. J., Rashleigh, B., Aretxabaleta, A. L., del Barrio, P., Grear, J. S., Harris, L. A., Lake, S. J., McCardell, G., O'Donnell, J., Ralston, D. K., Signell, R. P., Testa, J. M., Vaudrey, J. M. P., 2016. Progress and challenges in coupled hydrodynamic-ecological estuarine modeling. Estuaries and Coasts 39 (2), 311–332.

Geider, R. J., MacIntyre, H. L., Kana, T. M., 1997. A dynamic model of phytoplankton growth and acclimation: responses of the balanced growth rate and the chlorophyll a:carbon ratio to light, nutrient-limitation and temperature. Marine Ecology Progress Series 148, 187–200.

Geider, R. J., MacIntyre, H. L., Kana, T. M., 1998. A dynamic regulatory model of phytoplanktonic acclimation to light, nutrients, and temperature. Limnology and Oceanography 43 (4), 679–694.

Hagy, J. D., Murrell, M. C., 2007. Susceptibility of a northern Gulf of Mexico estuary to hypoxia: An analysis using box models. Estuarine Coastal and Shelf Science 74, 239–253.

Harvey, L. D. D., 2000. Upscaling in global change research. Climatic Change 44 (3), 225–263.

Hilborn, R., Mangel, M., 1997. The Ecological Detective: Confronting Models with Data. Princeton University Press, Princeton, New Jersey.

Hodur, R. M., 1997. The Naval Research Laboratory's Coupled Ocean/Atmosphere Mesoscale Prediction System (COAMPS). Monthly Weather Review 125, 1414–1430.

Howarth, R. W., Billen, G., Swaney, D., Townsend, A., Jaworski, N., Lajtha, K., Downing, J. A., Elmgren, R., Caraco, N., Jordan, T., Berendse, F., Freney, J., Kudeyarov, V., Murdoch, P., Zhao-Liang, Z., 1996. Regional nitrogen budgets and riverine N & P fluxes for the drainages to the North Atlantic Ocean: natural and human influences. Biogeochemistry 35 (1), 75–139.

Justíc, D., Legovíc, T., Rottini-Sandrini, L., 1987. Trends in oxygen content 1911–1984 and occurrence of benthic mortality in the northern Adriatic Sea. Estuarine, Coastal and Shelf Science 25 (4), 435–445.

Kirchner, J. W., 2006. Getting the right answers for the right reasons: Linking measurements, analyses, and models to advance the science of hydrology. Water Resources Research 42 (3), W03S04.

Lehman, J. T., Botkin, D. B., Likens, G. E., 1975. The assumptions and rationales of a computer model of phytoplankton population dynamics. Limnology and Oceanography 20 (3), 343–364.

Lehrter, J. C., Cebrian, J., 2010. Uncertainty propagation in an ecosystem nutrient budget. Ecological Applications 20 (2), 508–524.

Lehrter, J. C., Ko, D. S., Lowe, L., Penta, B., In press. Predicted effects of climate change on the severity of northern Gulf of Mexico hypoxia. In: Justic et al. (Ed.), Modeling Coastal Hypoxia: Numerical Simulations of Patterns, Controls, and Effect of Dissolved Oxygen Dynamics. Springer, New York.

Lehrter, J. C., Ko, D. S., Murrell, M. C., III, J. D. H., Schaeffer, B. A., Greene, R. M., Gould, R. W., Penta, B., 2013. Nutrient distributions, transports, and budgets on the inner margin of a river-dominated continental shelf. Journal of Geophysical Research 118 (10), 4822–4838.

Levins, R., 1966. The strategy of model building in population biology. American Scientist 54 (4), 421–431.

Lipton, D., Hicks, R., 2003. The cost of stress: low dissolved oxygen and eocnomic benefits of recreational striped bass (*Morone saxatilis* fishing in the Patuxent River. Estuaries 26 (2A), 310–315.

Lohrenz, S. E., Redalje, D. G., Cai, W. J., Acker, J., Dagg, M., 2008. A retrospective analysis of nutrients and phytoplankton productivity in the Mississippi River plume. Continental Shelf Research 28 (12), 1466–1475.

Martin, P. J., 2000. Description of the navy coastal ocean model version 1.0. Tech. Rep. NRL/FR/7322-00-9962, Naval Research Lab, Stennis Space Center, Mississippi.

Mateus, M. D., Franz, G., 2015. Sensitivity analysis in a complex marine ecological model. Water 7, 2060–2081.

Morrison, M., Morgan, M. S., 1999. Models as mediating agents. In: Morgan, M. S., Morrison, M. (Eds.), Models as Mediators. Cambridge University Press, Cambridge, p. 401.

Murrell, M. C., Beddick, D. L., Devereux, R., Greene, R. M., III, J. D. H., Jarvis, B. M., Kurtz, J. C., Lehrter, J. C., Yates, D. F., 2014. Gulf of mexico hypoxia research program data report: 2002-2007. Tech. Rep. EPA/600/R-13/257, US Environmental Protection Agency, Washington, DC.

Murrell, M. C., Stanley, R. S., Lehrter, J. C., Hagy, J. D., 2013. Plankton community respiration, net ecosystem metabolism, and oxygen dynamics on the Louisiana continental shelf: Implications for hypoxia. Continental Shelf Research 52, 27–38.

Nossent, J., Bauwens, W., 2012. Multi-variable sensitivity and identifiability analysis for a complex environmental model in view of integrated water quantity and water quality modeling. Water Science & Technology 65 (3), 539–549.

Obenour, D. R., Michalak, A. M., Scavia, D., 2015. Assessing biophysical controls on Gulf of Mexico hypoxia through probabilistic modeling. Ecological Applications 25 (2), 492–505.

Omlin, M., Brun, R., Reichert, P., 2001a. Biogeochemical model of Lake Zürich: sensitivity, identifiability and uncertainty analysis. Ecological Modelling 141 (1-3), 105–123.

Omlin, M., Reichert, P., Forster, R., 2001b. Biogeochemical model of Lake Zürich: model equations and results. Ecological Modelling 141 (1-3), 77–103.

Paerl, H. W., Pinckney, J. L., Fear, J. M., Peierls, B. L., 1998. Ecosystem responses to internal and watershed organic matter loading: consequences for hypoxia in the eutrophying Neuse River Estuary, North Carolina, USA. Marine Ecology Progress Series 166, 17–25.

Pauer, J. J., Feist, T. J., Anstead, A. M., DePetro, P. A., Melendez, W., Lehrter, J. C., Murrell, M. C., Zhang, X., Ko, D. S., 2016. A modeling study examining the impact of nutrient boundaries on primary production on the Louisiana continental shelf. Ecological Modelling 328, 136–147.

Penta, B., Lee, Z., Kudela, R. M., Palacios, S. L., Gray, D. J., Jolliff, J. K., Shulman, I. G., 2008. An underwater light attenuation scheme for marine ecosystem models. Optical Express 16 (21), 16581–16591.

Penta, B., Lee, Z., Kudela, R. M., Palacios, S. L., Gray, D. J., Jolliff, J. K., Shulman, I. G., 2009. An underwater light attenuation scheme for marine ecosystem models: errata. Optical Express 17 (25), 23351–23351.

Petrucci, G., Bonhomme, C., 2014. The dilemma of spatial representation for urban hydrology semi-distributed modelling: trade-offs among complexity, calibration and geographical data. Journal of Hydrology 517, 997–1007.

Platt, T., Gallegos, C. L., Harrison, W. G., 1980. Photoinhibition of photosynthesis in natural assemblages of marine phytoplankton. Journal of Marine Research 38, 687–701.

Rabalais, N. N., Turner, R. E., Scavia, D., 2002. Beyond science into policy: Gulf of Mexico hypoxia and the Mississippi river. BioScience 52 (2), 129–142.

RDCT (R Development Core Team), 2016. R: A language and environment for statistical computing, v3.3.1. R Foundation for Statistical Computing, Vienna, Austria. http://www.R-project.org.

Reckhow, K. H., Clements, J. T., Dodd, R. C., 1990. Statistical evaluation of mechanistic water-quality models. Journal of Environmental Engineering 116 (2), 250–268.

Refsgaard, J. C., van der Sluijs, J. P., Højberg, A. L., Vanrolleghem, P. A., 2007. Uncertainty in the environmental modelling process - a framework and guidance. Environmental Modelling & Software 22 (11), 1543–1556.

Reichert, P., Omlin, M., 1997. On the usefulness of over parameterized ecological models. Ecological Modelling 95 (2), 289–299.

Roelke, D. L., 2000. Copepod food-quality threshold as a mechanism influencing phytoplankton succession and accumulation of biomass, and secondary productivity: a modeling study with management implications. Ecological Modelling 134, 245–274.

Scavia, D., Justic, D., Bierman, V. J., 2004. Reducing hypoxia in the Gulf of Mexico: Advice from three models. Estuaries 27 (3), 419–425.

Snowling, S. D., Kramer, J. R., 2001. Evaluating modelling uncertainty for model selection. Ecological Modelling 138, 17–30.

Soetaert, K., Petzoldt, T., 2010. Inverse modelling, sensitivity, and Monte Carlo analysis in R using package FME. Journal of Statistical Software 33 (3), 1–28.

Wade, A. J., Jackson, B. M., Butterfield, D., 2008. Over-parameterised, uncertain 'mathematical marionettes' - how can we best use catchment water quality models? An example of an 80-year catchment-scale nutrient balance. Science of the Total Environment 400 (1-3), 52–74.

Wagener, T., Boyle, D. P., Lees, M. J., Wheater, H. S., Gupta, H. V., Sorooshian, S., 2001a. A framework for development and application of hydrological models. Hydrology and Earth System Sciences 5 (1), 13–26.

Wagener, T., Lees, M. J., Wheater, H. S., 2001b. A toolkit for the development and application of parsimonious hydrological models. In: Singh, V. P., Meyer, D. K. F. S. P. (Eds.), Mathematical Models of Small Watershed Hydrology and Applications - Volume 2. Water Resources Publications LLC, USA, pp. 91–140.

Warner, J. C., Geyer, W. R., Lerczak, J. A., 2005. Numerical modeling of an estuary: a comprehensive skill assessment. Journal of Geophysical Research: Oceans 110 (C5), 13.

Wheater, H. S., Bishop, K. H., Beck, M. B., 1986. The identification of conceptual hydrological models for surface water acidification. Hydrological Processes 1 (1), 89–109.

Wiseman, W. J., Rabalais, N. N., Turner, R. E., Dinnel, S. P., MacNaughton, A., 1997. Seasonal and interannual variability within the Louisiana coastal current: stratification and hypoxia. Journal of Marine Systems 12 (1-4), 237–248.

Ye, W., Bates, B. C., Viney, N. R., Sivapalan, M., Jakeman, A. J., 1997. Performance of conceptual rainfall-runoff models in low yielding ephemeral catchments. Water Resources Research 33 (1), 153–166.

Zhao, L., Chen, C., Vallino, J., Hopkinson, C., Beardsley, R. C., Lin, H., Lerczak, J., 2010. Wetland-estuarine-shelf interactions on the Plum Island Sound and Merrimack River in the Massachusetts coast. Journal of Geophysical Research 115 (C10), 13.

Table 1: Initial conditions that were varied to evaluate effects of observational uncertainty on parameter sensitivity. April and September values are based on seasonal averages from water quality samples of the LCS. All units are μmol L^{-1}.

Variables	Default	April	September
Dissolved Inorganic Carbon	2.13×10^3	2.1×10^3	2.13×10^3
Ammonium	1.09	1.79	0.35
Nitrate	71.4	3.75	2.04
Dissolved Oygen	172	194.47	152.57
Phosphate	1.81	0.23	0.42
Silica	71.4	5.84	9.77

Table 2: Model switches that were used to evaluate effects of structural uncertainty on parameter sensitivity. Complete details and equations are provided as supplementary material to Lehrter et al. in press.

Switch type	Default	Complex
Temperature	sigmoidal (Eldridge and Roelke, 2010)	Arrenhius (Geider et al., 1997)
Uptake	Michaelis-Menten (Dugdale and Goering, 1967)	Geider (Lehman et al., 1975; Geider et al., 1998)
Quota	Droop (Droop, 1973)	Flynn (Flynn, 2003)
Chla:C	regression (Murrell et al., 2014)	Cloern (Cloern et al., 1995)
Photosynthesis	photoinhibition (Platt et al., 1980)	nutrient dependent
Specific growth rate	Leibig's minimum	nutrient dependent

Table 3: Sensitivity of O_2 to perturbations of individual parameters. Sensitivities are based on a 50% increase from the initial parameter value, where $L1$ summarizes differences in model output from the default (see eq. (2)). Parameters that did not affect O_2 are not shown. Parameters are grouped by categories as optics, temperature, phytoplankton, zooplankton, and organic matter.

Description	Parameter	L1
Optics		
Chla specific absorption at 490 nm	*astar490*	7.51×10^{-4}
OMZ specific absorption at 490 nm	*astarOMZ*	4.92×10^{-5}
OMA specific absorption at 490 nm	*astarOMA*	4.39×10^{-5}
Temperature		
Optimum temperature for growth(C)	$Tref(nospA+nospZ)_{p1}$	0.02
Phytoplankton		
maximum growth rate	*umax*	0.05
mortality coefficient	*mA*	0.02
initial slope of the photosynthesis-irradiance relationship	*alpha*	0.02
edibility vector for Z1	*ediblevector(Z1)*	0.02
phytoplankton carbon/cell	*Qc*	0.01
phytoplankton growth respiration coefficient	*respg*	8.36×10^{-3}
N-uptake rate measured at umax	*vmaxN*	8.12×10^{-3}
phytoplankton basal respiration coefficient	*respb*	6.94×10^{-3}
Phytoplankton threshold for grazing, is multiplied by VOLcell	*Athresh*	4.57×10^{-3}
minimum N cell-quota	*QminN*	4.32×10^{-3}
P-uptake rate measured at umax	*vmaxP*	4.27×10^{-3}
coefficient for non-limiting nutrient	*aN*	4.23×10^{-3}
phytoplankton volume/cell	*volcell*	4.13×10^{-3}
half-saturation constant for P	*Kp*	2.9×10^{-3}
half-saturation constant for N	*Kn*	2.77×10^{-4}
minimum P cell-quota	*QminP*	8.34×10^{-8}
Zooplankton		
half saturation coefficient for grazing	*ZKa*	0.05
zooplankton nitrogen/individual	*ZQn*	0.02
Zooplankton mortality constant for quadratic mortality	*Zm*	0.02
maximum growth rate of zooplankton	*Zumax*	0.02
assimilation efficiency as a fraction of ingestion	*Zeffic*	0.01
proportion of grazed phytoplankton lost to sloppy feeding	*Zslop*	7.78×10^{-3}
Zooplankton growth-dependent respiration factor	*Zrespg*	5.32×10^{-3}
Zooplankton biomass-dependent respiration factor	*Zrespb*	2.96×10^{-3}
zooplankton carbon/individual	*ZQc*	9.38×10^{-5}
zooplankton phosphorus/individual	*ZQp*	3.69×10^{-5}
Organic Matter		
turnover rate for OM1A and OM1Z	*KG1*	6.15×10^{-3}
turnover rate for OM2A and OM2Z	*KG2*	3.14×10^{-3}
O2 concentration that inhibits denitrification	*KstarO2*	3.04×10^{-3}
decay rate of CDOM, 1/day	*KGcdom*	2.98×10^{-3}
half-saturation concentration for O2 utilization	*KO2*	5.85×10^{-4}
half-saturation concentration for NO3 used in denitrification	*KNO3*	5.8×10^{-4}
maximum rate of nitrification per day	*nitmax*	4.99×10^{-4}
NH4 rate constant for nitrification	*KNH4*	4.17×10^{-4}

*Temperature parameters apply separately to phytoplankton (*p1*, one group) or zooplankton (*z1*, one group), denoted by subscripts

Table 4: Parameter identifiability (as γ, eq. (3)) by category for relevant state variables. Selections followed the first heuristic where parameters were selected within categories from most to least sensitive until $\gamma > 15$. Rank describes the relative parameter sensitivity in each category for each state variable. Duplicate parameters and ranks in the first two columns apply only to γ values in the same row (i.e., parameter ranks vary for each variable).

Parameter	Rank	Ammonium	Chl-a	O_2	Irradiance	Nitrate	POM	DOM	Phosphate
Optics									
astar490	1	1	1	1	1	1	1	1	1
astarOMA	2	7.33	5.42	-	7.87	5.36	-	-	7.78
astarOMZ	2	-	-	1.39	-	-	-	4.73	-
astarOMA	3	-	-	3.87	-	-	-	10.04	-
astarOMZ	3	7.58	5.51	-	7.87	6.02	-	-	7.91
Organic Matter									
KG1	1	-	-	1	-	-	-	1	1
KG2	1	-	-	-	1	-	-	-	-
KGcdom	1	-	1	-	-	1	-	-	-
KstarO2	1	-	-	-	-	-	1	-	-
nitmax	1	1	-	-	-	-	-	-	-
KG1	2	-	1.12	-	-	1.93	-	-	-
KG2	2	-	-	6	-	-	-	13.43	-
KGcdom	2	-	-	-	1.39	-	-	-	1.47
KNH4	2	4.03	-	-	-	-	-	-	-
KG1	3	4.09	-	-	-	-	-	-	-
KG2	3	-	-	-	-	8.19	-	-	-
KGcdom	3	-	-	-	-	-	-	13.75	-
KO2	3	-	-	-	11.96	-	-	-	14.07
KstarO2	3	-	-	6.04	-	-	-	-	-
KGcdom	4	4.19	-	6.12	-	-	-	-	-
KO2	4	-	-	-	-	-	-	14.68	-
KstarO2	4	-	-	-	-	10.65	-	-	14.08
KO2	5	9.47	-	8.61	-	-	-	-	-
Phytoplankton									
mA	1	1	1	-	1	-	-	-	1
umax	1	-	-	1	-	1	1	1	-
ediblevector(Z1)	2	1.13	1.17	-	-	-	-	-	1.15
mA	2	-	-	1.19	-	1.29	-	-	-
Qc	2	-	-	-	-	-	11.57	-	-
umax	2	-	-	-	1.21	-	-	-	-
vmaxP	2	-	-	-	-	-	-	7.45	-
alpha	3	-	-	1.44	-	1.98	-	-	-
ediblevector(Z1)	3	-	-	-	2.9	-	-	-	-
umax	3	2.73	2.11	-	-	-	-	-	3.26
alpha	4	3.55	4.57	-	-	-	-	-	-
ediblevector(Z1)	4	-	-	2.09	-	4.09	-	-	-
Qc	4	-	-	-	-	-	-	-	4.98
vmaxN	4	-	-	-	4.9	-	-	-	-
alpha	5	-	-	-	-	-	-	-	10.11
Qc	5	-	-	2.9	-	-	-	-	-
vmaxN	5	8.14	-	-	-	-	-	-	-
Athresh	6	11.27	-	-	-	-	-	-	-
respg	6	-	-	3.41	-	-	-	-	-
vmaxN	7	-	-	3.97	-	-	-	-	-
Zooplankton									
ZKa	1	-	-	1	-	1	1	1	-
Zumax	1	1	1	-	1	-	-	-	1
ZKa	2	-	4.31	-	5.43	-	-	-	7.3
ZQn	2	-	-	3.18	-	6.32	9.76	8.54	-
Zm	3	-	-	4.57	-	-	-	-	-
Zumax	3	-	-	-	-	6.93	-	-	-
Zm	4	-	-	-	-	11.86	-	-	-
Zumax	4	-	-	5.2	-	-	-	-	-

Table 5: Parameter identifiability (as γ, eq. (3)) for relevant state variables. Selections followed the second heuristic where parameters were selected independent of category from most to least sensitive (L1, eq. (2)), until $\gamma > 15$. Rank describes the relative parameter sensitivity in each category for each state variable (O: optics, OM: organic matter, P: phytoplankton, T: temperature, Z: zooplankton). See Fig. 7 for a graphical illustration.

Selections by state variable	Parameter	L1	Rank	γ
Ammonium				
1	mA	8.49	1_P	1
2	$nitmax$	1.54	1_{OM}	1.16
3	$Zumax$	1.42	1_Z	2.9
Chlorophyll				
1	mA	13.94	1_P	1
2	$Zumax$	1.02	1_Z	1.18
Dissolved Oxygen				
1	$umax$	0.05	1_P	1
2	ZKa	0.05	1_Z	2.17
3	mA	0.02	2_P	2.31
4	$Tref(nospA+nospZ)_{p1}$	0.02	1_T	2.37
5	ZQn	0.02	2_Z	4.69
6	$alpha$	0.02	3_P	4.91
7	Zm	0.02	3_Z	6.73
8	$Zumax$	0.02	4_Z	6.81
DOM				
1	mA	14.25	1_P	1
2	$Tref(nospA+nospZ)_{p1}$	1.48	1_T	1.05
3	$umax$	1.11	2_P	2.46
4	$Zumax$	1.01	1_Z	2.91
Irradiance				
1	ZKa	0.13	1_Z	1
2	$umax$	0.09	1_P	4.41
3	ZQn	0.06	2_Z	7.54
4	mA	0.05	2_P	8.17
5	$KGcdom$	0.05	1_{OM}	9.44
6	$alpha$	0.04	3_P	9.66
7	$Zumax$	0.04	3_Z	10.79
Nitrate				
1	$umax$	8.49	1_P	1
Phosphate				
1	ZKa	1.47	1_Z	1
2	$umax$	0.78	1_P	11.45
3	$vmaxP$	0.59	2_P	11.48
4	ZQn	0.5	2_Z	13.74
POM				
1	mA	7.22	1_P	1
2	$Zumax$	0.96	1_Z	1.15
3	$KG1$	0.92	1_{OM}	3.87

Table 6: Parameter identifiability (as γ, eq. (3)) for relevant state variables. Selections followed the third heuristic where parameters were selected equally within each category from most to least sensitive (L1, eq. (2)), until $\gamma > 15$. Rank describes the relative parameter sensitivity in each category for each state variable (O: optics, OM: organic matter, P: phytoplankton, T: temperature, Z: zooplankton).

Selections by state variable	Parameter	L1	Rank	γ
Ammonium				
1	mA	8.49	1_P	1
2	$nitmax$	1.54	1_{OM}	1.16
3	$Zumax$	1.42	1_Z	2.9
4	$Tref(nospA+nospZ)_{p1}$	0.79	1_T	3.46
5	$astar490$	0.03	1_O	4.25
Chlorophyll				
1	mA	13.94	1_P	1
2	$Zumax$	1.02	1_Z	1.18
3	$Tref(nospA+nospZ)_{p1}$	0.6	1_T	2.62
4	$KGcdom$	0.07	1_{OM}	3.24
5	$astar490$	0.02	1_O	5.98
Dissolved Oxygen				
1	$umax$	0.05	1_P	1
2	ZKa	0.05	1_Z	2.17
3	$Tref(nospA+nospZ)_{p1}$	0.02	1_T	2.29
4	$KG1$	6.15×10^{-3}	1_{OM}	3.85
5	$astar490$	7.51×10^{-4}	1_O	3.89
6	mA	0.02	2_P	4.42
7	ZQn	0.02	2_Z	5.22
DOM				
1	mA	14.25	1_P	1
2	$Tref(nospA+nospZ)_{p1}$	1.48	1_T	1.05
3	$Zumax$	1.01	1_Z	2.61
4	$KG2$	0.94	1_{OM}	3.39
5	$astar490$	0.04	1_O	4.46
6	$umax$	1.11	2_P	6.02
7	ZKa	0.88	2_Z	9.21
Irradiance				
1	ZKa	0.13	1_Z	1
2	$umax$	0.09	1_P	4.41
3	$KGcdom$	0.05	1_{OM}	4.5
4	$Tref(nospA+nospZ)_{p1}$	0.03	1_T	4.5
5	$astar490$	0.02	1_O	6.9
6	ZQn	0.06	2_Z	10.63
7	mA	0.05	2_P	11.21
8	$KG1$	3.96×10^{-3}	2_{OM}	14.65
9	$astarOMA$	1.47×10^{-3}	2_O	14.72
Nitrate				
1	$umax$	8.49	1_P	1
Phosphate				
1	ZKa	1.47	1_Z	1
2	$umax$	0.78	1_P	11.45
3	$Tref(nospA+nospZ)_{p1}$	0.16	1_T	13.71
4	$KG1$	0.14	1_{OM}	14.64
POM				
1	mA	7.22	1_P	1
2	$Zumax$	0.96	1_Z	1.15
3	$KG1$	0.92	1_{OM}	3.87
4	$Tref(nospA+nospZ)_{p1}$	0.86	1_T	3.93
5	$astar490$	0.03	1_O	5.81

Table 7: Changes in mean sensitivity of state variables by parameter categories to different initial conditions and structural components of the model. Changes show the difference in average sensitivity from results using the default model setup. Sensitivities are based on average $L1$ (see eq. (2)) values of the state variables to changes in parameters in each parameter category. Increases in average sensitivity are in bold. Medians and ranges of sensitivity values for the different conditions are shown in Fig. 8.

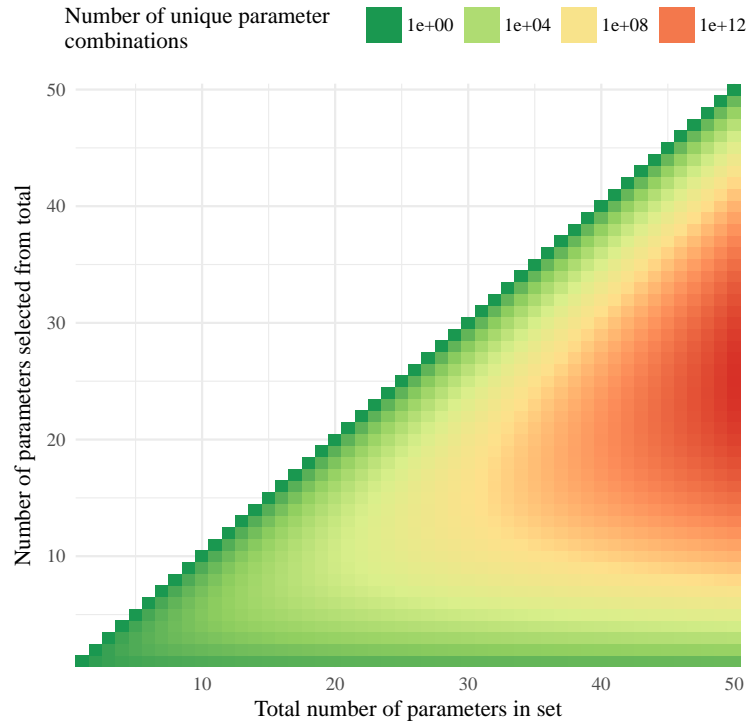| State variables by parameter category		Change		
	Default sensitivity	Initial: April	Initial: September	Structure: complex
Optics				
Ammonium	0.01	-9.13×10^{-3}	-8.37×10^{-3}	-7.7×10^{-3}
Chlorophyll	8.77×10^{-3}	-6.79×10^{-3}	-6.3×10^{-3}	-7.33×10^{-3}
Dissolved Oxygen	2.81×10^{-4}	-2.11×10^{-4}	-1.46×10^{-4}	-1.93×10^{-4}
Irradiance	9.1×10^{-3}	$\mathbf{2.56 \times 10^{-3}}$	$\mathbf{3.1 \times 10^{-3}}$	$\mathbf{1.57 \times 10^{-3}}$
Nitrate	7.72×10^{-3}	-6.46×10^{-3}	-6.2×10^{-3}	-6.8×10^{-3}
POM	0.01	-9.06×10^{-3}	-8.49×10^{-3}	-8.56×10^{-3}
DOM	0.02	-0.01	-0.01	-0.01
Phosphate	3.35×10^{-3}	-2.53×10^{-3}	-2.15×10^{-3}	-3.04×10^{-3}
Organic Matter				
Ammonium	0.31	**0.08**	**0.04**	-2.22×10^{-4}
Chlorophyll	0.02	**0.12**	**0.14**	-0.01
Dissolved Oxygen	2.17×10^{-3}	-6.75×10^{-4}	$\mathbf{2.32 \times 10^{-4}}$	-1.05×10^{-3}
Irradiance	6.63×10^{-3}	$\mathbf{5.34 \times 10^{-3}}$	$\mathbf{6.79 \times 10^{-3}}$	-2.99×10^{-4}
Nitrate	0.12	**0.06**	**0.09**	-0.1
POM	0.13	**0.15**	**0.12**	**0.04**
DOM	0.14	**0.07**	**0.17**	**0.05**
Phosphate	0.03	**0.04**	**0.06**	-0.02
Phytoplankton				
Ammonium	0.8	-0.02	**0.3**	**65.98**
Chlorophyll	1.14	**1.23**	**4.38**	**104.24**
Dissolved Oxygen	0.01	-4.58×10^{-4}	$\mathbf{2.31 \times 10^{-3}}$	$\mathbf{3.44 \times 10^{-4}}$
Irradiance	0.02	-2.04×10^{-3}	$\mathbf{1.83 \times 10^{-3}}$	$\mathbf{7.53 \times 10^{-3}}$
Nitrate	0.74	-0.43	-0.45	-0.64
POM	0.76	**0.17**	**0.46**	**55.11**
DOM	1.28	**0.34**	**1.15**	**128.93**
Phosphate	0.17	**0.03**	**0.05**	-0.14
Temperature				
Ammonium	0.79	-0.69	-0.69	**272.31**
Chlorophyll	0.6	-0.47	-0.45	**114.51**
Dissolved Oxygen	0.02	-0.02	-0.02	-0.01
Irradiance	0.03	-0.02	-0.02	**0.01**
Nitrate	0.3	-0.15	-0.16	-0.19
POM	0.86	-0.68	-0.69	**215.17**
DOM	1.48	-1.21	-1.2	**900.26**
Phosphate	0.16	-0.11	-0.09	-0.11
Zooplankton				
Ammonium	0.47	-0.45	-0.44	-0.16
Chlorophyll	0.39	-0.26	-0.23	-0.2
Dissolved Oxygen	0.01	-0.01	-8.68×10^{-3}	-6.96×10^{-3}
Irradiance	0.03	-0.02	-0.02	-0.01
Nitrate	1.06	-1.02	-1.02	-0.98
POM	0.37	-0.27	-0.28	-0.18
DOM	0.39	-0.3	-0.28	-0.18
Phosphate	0.31	-0.19	-0.17	-0.27

Fig. 1: Examples of unique parameter combinations from different parameter sets and number of selected parameters. The number of combinations are shown for increasing numbers of selected parameters from the total in the set, where 50 parameter sets are shown each with one through 50 total parameters. Note that the number of unique combinations is shown as the natural-log.
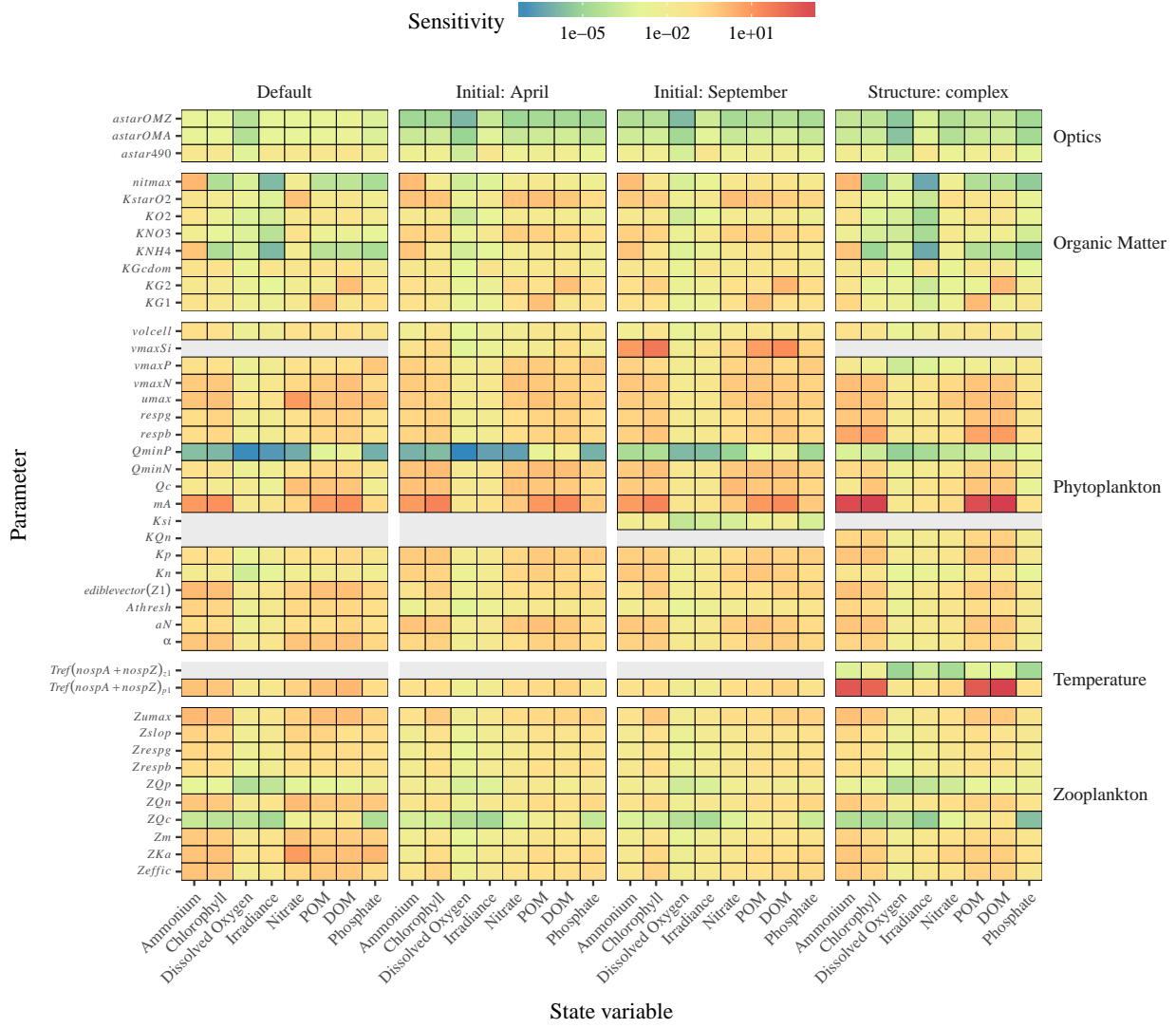
Fig. 2: Sensitivity values (L1, eq. (2)) of all state variables to changes in parameter values using default conditions, changes in initial conditions (April, September seasonal means, Table 1), and changes in structural complexity (Table 2). Parameters are grouped by category: optics, organic matter, phytoplankton, zooplankton, temperature, and zoplankton. See Table 3 for L1 values for O_2 and Tables S1 to S7 for the other state variables.
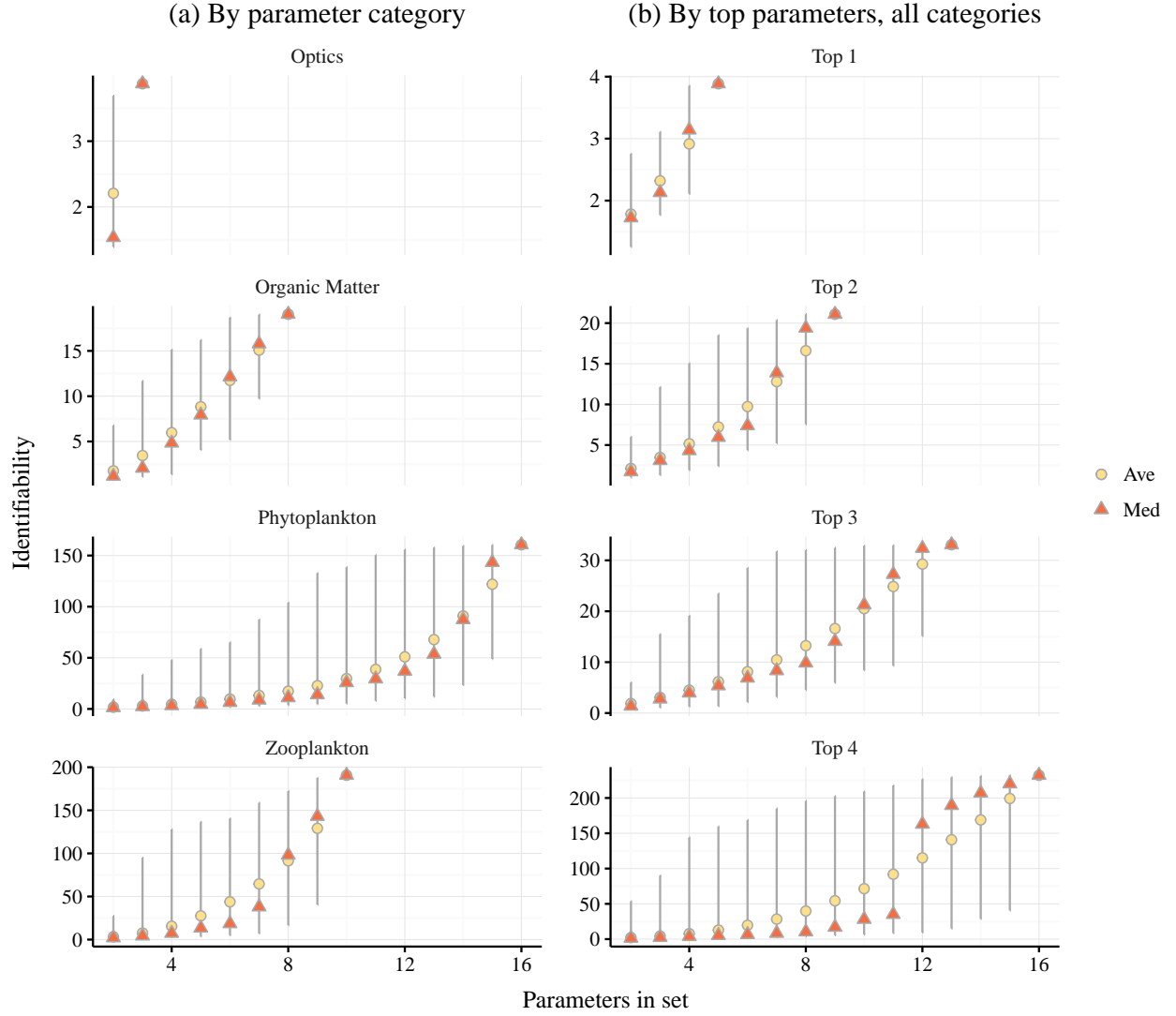
Fig. 3: Identifiability (as γ, eq. (3)) of parameter subsets for O_2. Plots in (a) show identifiability by parameter categories and (b) shows identifiability by selecting the top 1 through 4 parameters in all categories. Lines represent identifiability ranges for the possible combinations given the number of parameters in the set. The temperature category is not shown because O_2 was sensitive to only one parameter (i.e., $\gamma = 1$).
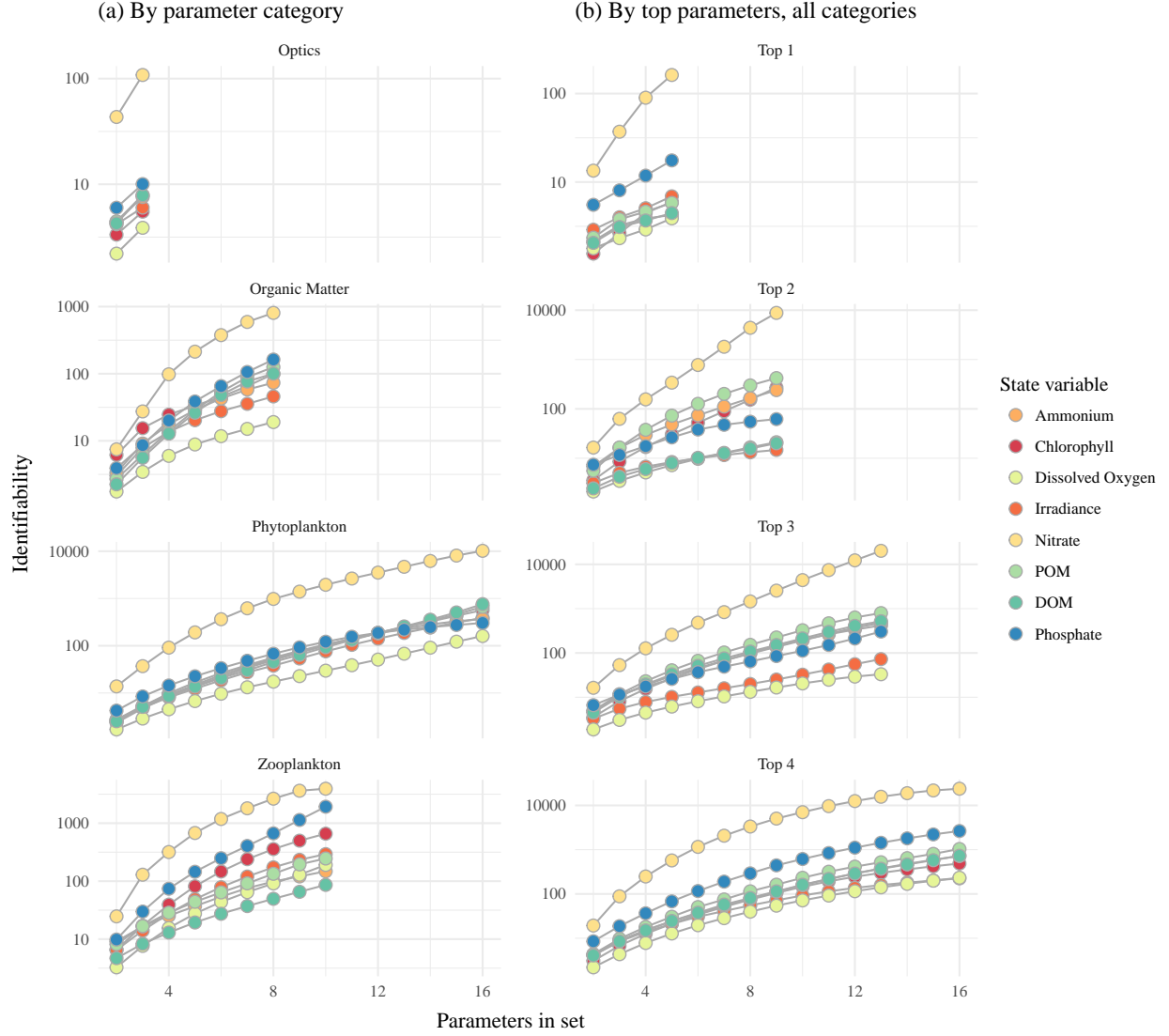
Fig. 4: Average identifiability (as γ, eq. (3)) of parameter subsets for all state variables. Plots in (a) show identifiability by parameter categories and (b) shows identifiability by selecting the top 1 through 4 parameters in all categories. Identifiability was averaged for all combinations in a parameter set to evaluate relative differenes between state variables. The temperature category is not shown because all state variables were sensitive to only one parameter (i.e., $\gamma = 1$).
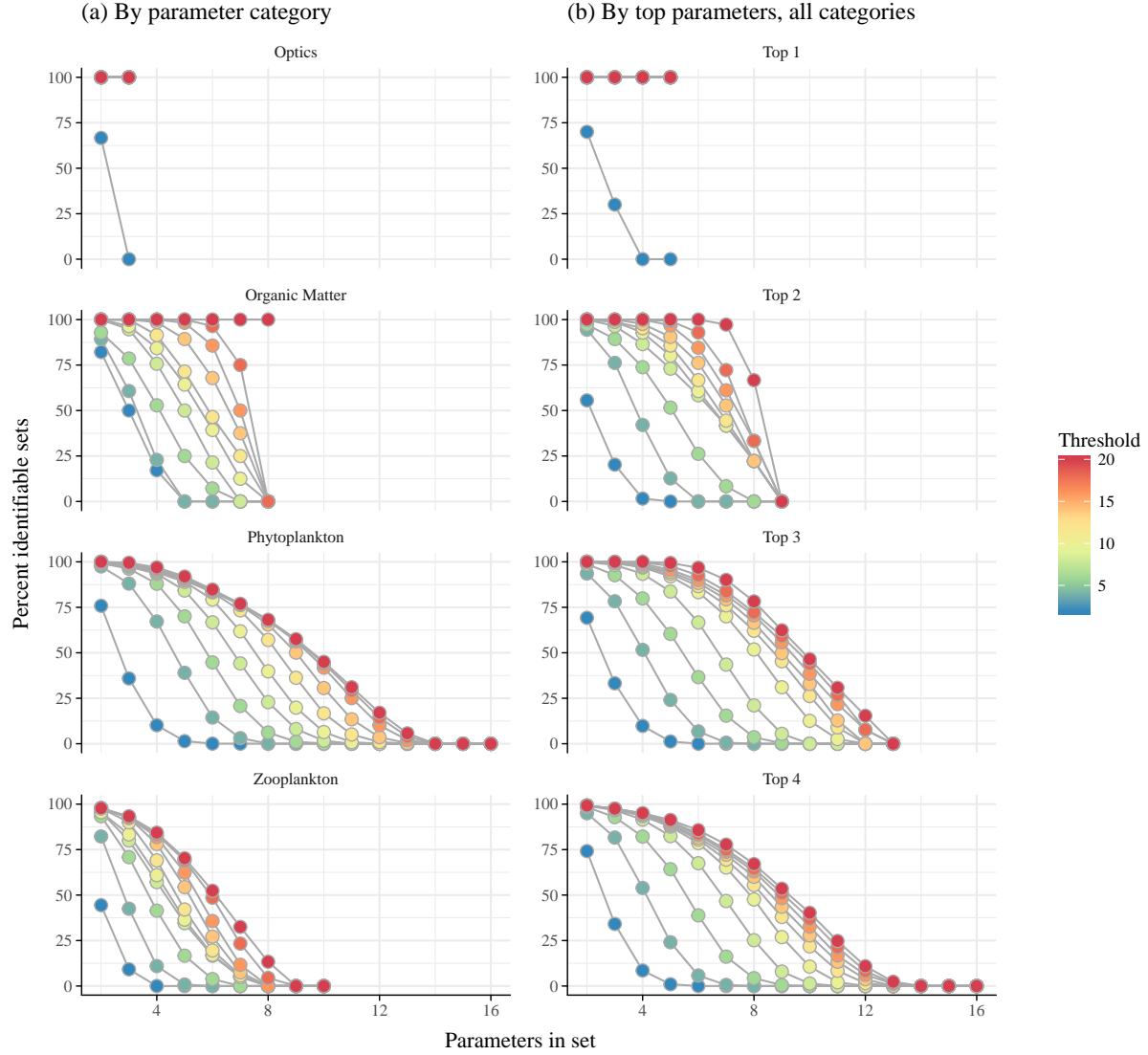
Fig. 5: Percent of identifiable parameter sets for O_2 at different γ thresholds, selection criteria, and total number of parameters in the set. Thresholds varied from $\gamma = 2$ to 20 such that sets with γ below a threshold were considered identifiable relative to the value. Plots in (a) show percent of identifiable sets by selecting parameters within categories and (b) shows percent identifiable by selecting from the top 1 through 4 parameters in all categories. Percent identifiable was based on all sets in Fig. 3.
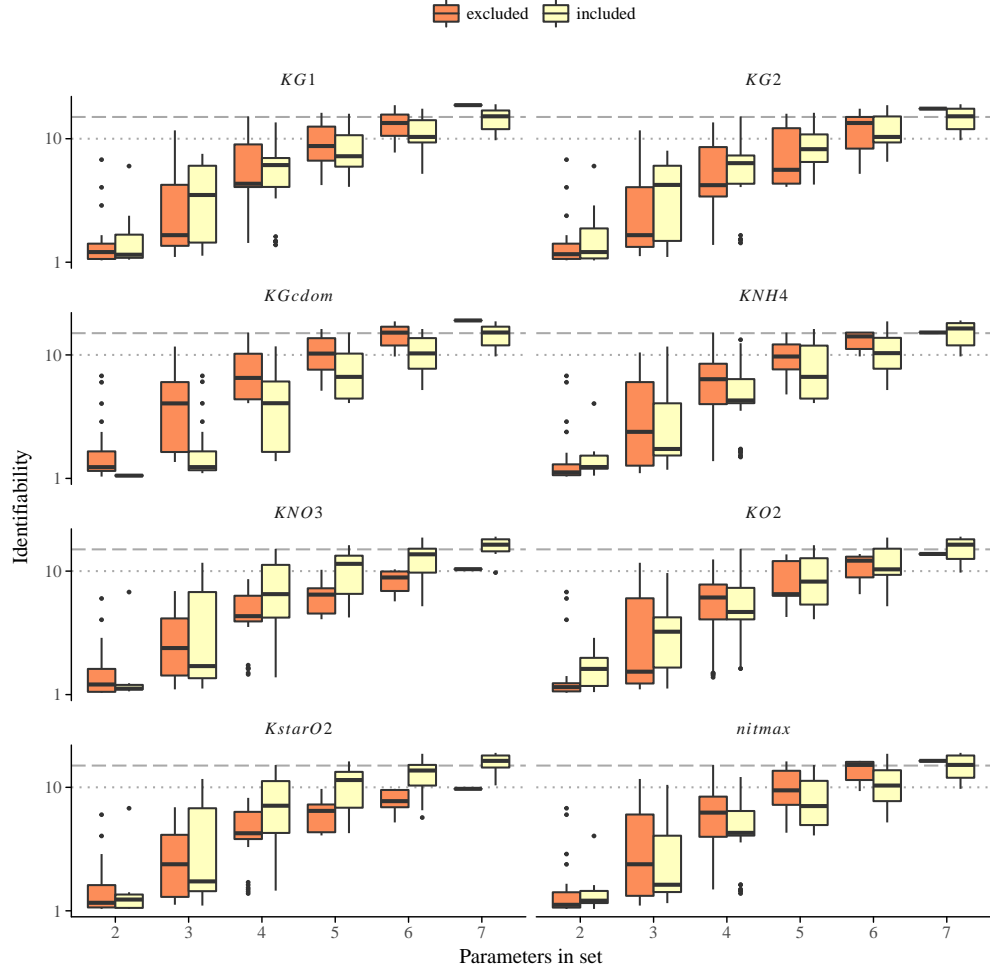
Fig. 6: Identifiability (as γ, eq. (3)) for O_2 of organic matter parameters for subset combinations in Fig. 3. Identifiability is evaluated for subsets that excluded and included the parameters at the top of each plot. Identifiability of including all eight parameters is in Fig. 3. Grey lines indicate potential thresholds at $\gamma = 10, 15$ for maximum acceptable identifiability.
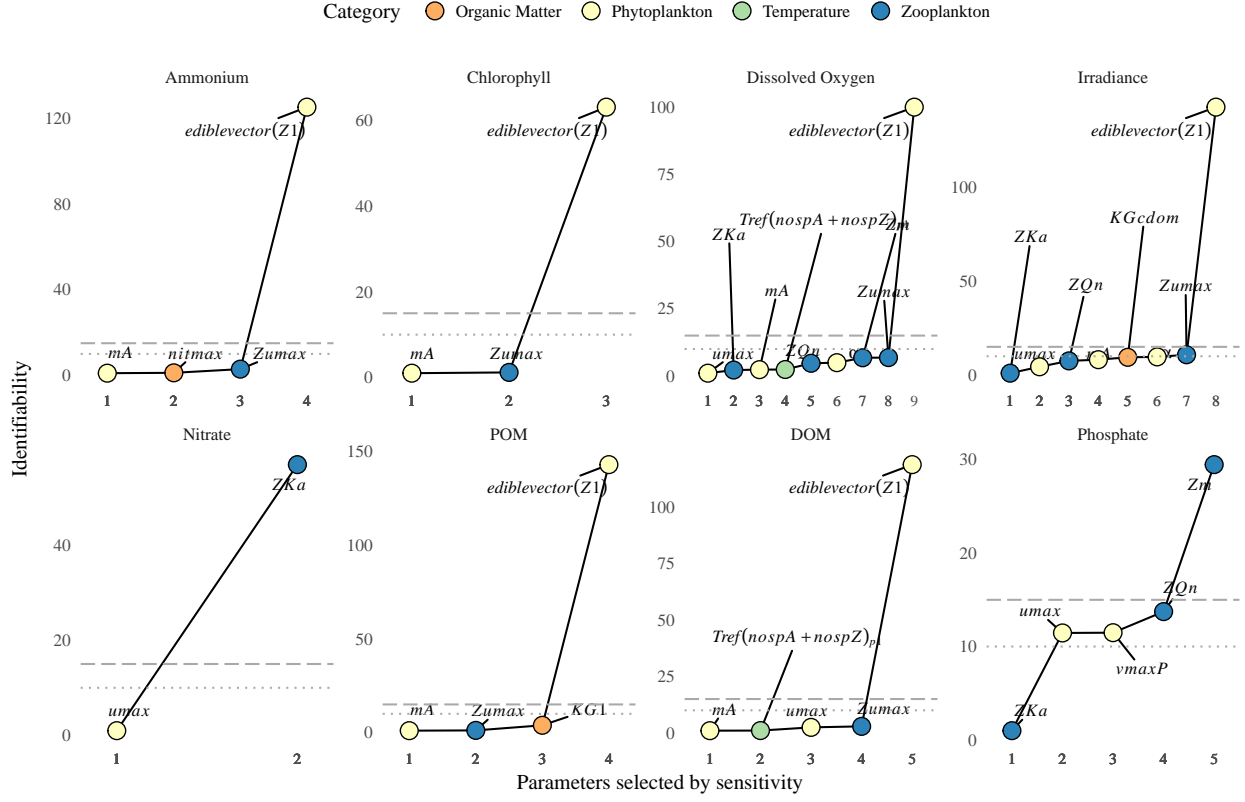
Fig. 7: Identifiability (as γ, eq. (3)) of selecting parameters for all state variables. Parameters are selected by decreasing sensitivity independent of parameter categories. Grey lines indicate potential thresholds at $\gamma = 10, 15$ for maximum acceptable identifiability. Selection stops after $\gamma > 15$.
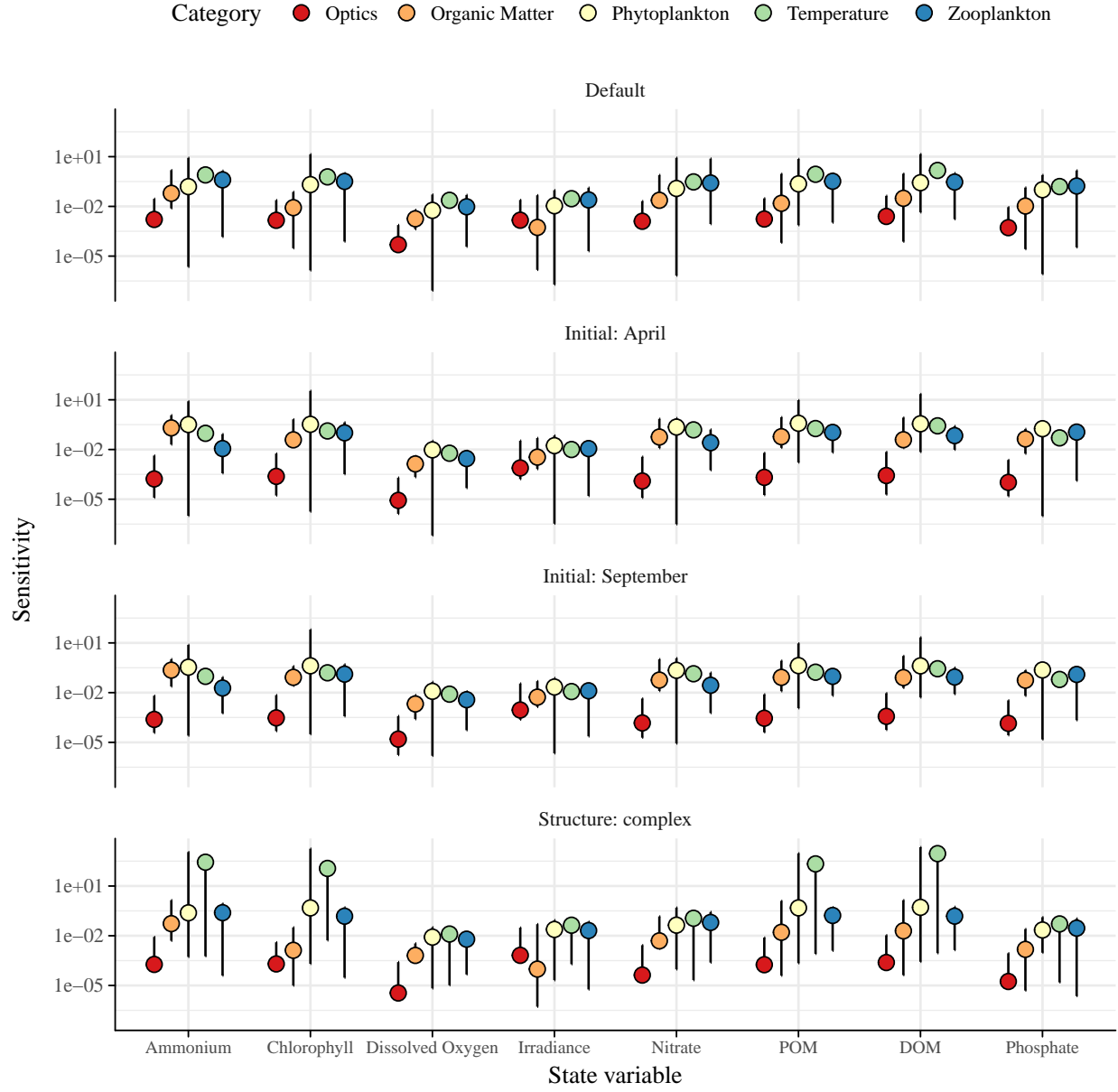
Fig. 8: Summaries of changes in parameter sensitivity values (L1, eq. (2)) from the default model conditions. Sensitivity was re-evaluated using initial conditions as seasonal means for April and September, and added structural complexity. Sensitivity is summarized as the minimum, median, and maximum for each state variable separated by parameter categories. Changes in average sensitivity from the default model conditions are in Table 7.

Table S1: Sensitivity of ammonium to perturbations of individual parameters. Sensitivities are based on a 50% increase from the initial parameter value, where $L1$ summarizes differences in model output from the default (see eq. (2)). Parameters that did not affect ammonium are not shown. Parameters are grouped by categories as optics, temperature, phytoplankton, zooplankton, and organic matter.

Description	Parameter	L1
Optics		
Chla specific absorption at 490 nm	*astar490*	0.03
OMA specific absorption at 490 nm	*astarOMA*	1.63×10^{-3}
OMZ specific absorption at 490 nm	*astarOMZ*	1.5×10^{-3}
Temperature		
Optimum temperature for growth(C)	$Tref(nospA{+}nospZ)_{p1}$	0.79
Phytoplankton		
mortality coefficient	*mA*	8.49
edibility vector for Z1	*ediblevector(Z1)*	1.32
maximum growth rate	*umax*	0.65
initial slope of the photosynthesis-irradiance relationship	*alpha*	0.6
N-uptake rate measured at umax	*vmaxN*	0.46
Phytoplankton threshold for grazing, is multiplied by VOLcell	*Athresh*	0.29
coefficient for non-limiting nutrient	*aN*	0.17
phytoplankton growth respiration coefficient	*respg*	0.16
phytoplankton basal respiration coefficient	*respb*	0.15
half-saturation constant for P	*Kp*	0.14
phytoplankton volume/cell	*volcell*	0.14
minimum N cell-quota	*QminN*	0.1
P-uptake rate measured at umax	*vmaxP*	0.1
phytoplankton carbon/cell	*Qc*	0.03
half-saturation constant for N	*Kn*	0.01
minimum P cell-quota	*QminP*	2.24×10^{-6}
Zooplankton		
maximum growth rate of zooplankton	*Zumax*	1.42
assimilation efficiency as a fraction of ingestion	*Zeffic*	0.76
half saturation coefficient for grazing	*ZKa*	0.74
zooplankton nitrogen/individual	*ZQn*	0.62
Zooplankton mortality constant for quadratic mortality	*Zm*	0.5
proportion of grazed phytoplankton lost to sloppy feeding	*Zslop*	0.3
Zooplankton growth-dependent respiration factor	*Zrespg*	0.22
Zooplankton biomass-dependent respiration factor	*Zrespb*	0.16
zooplankton phosphorus/individual	*ZQp*	1.07×10^{-3}
zooplankton carbon/individual	*ZQc*	1.44×10^{-4}
Organic Matter		
maximum rate of nitrification per day	*nitmax*	1.54
NH4 rate constant for nitrification	*KNH4*	0.66
turnover rate for OM1A and OM1Z	*KG1*	0.07
decay rate of CDOM, 1/day	*KGcdom*	0.07
half-saturation concentration for O2 utilization	*KO2*	0.06
O2 concentration that inhibits denitrification	*KstarO2*	0.05
turnover rate for OM2A and OM2Z	*KG2*	0.03
half-saturation concentration for NO3 used in denitrification	*KNO3*	7.55×10^{-3}

Table S2: Sensitivity of chl-a to perturbations of individual parameters. Sensitivities are based on a 50% increase from the initial parameter value, where $L1$ summarizes differences in model output from the default (see eq. (2)). Parameters that did not affect chl-a are not shown. Parameters are grouped by categories as optics, temperature, phytoplankton, zooplankton, and organic matter.

Description	Parameter	L1
Optics		
Chla specific absorption at 490 nm	$astar490$	0.02
OMA specific absorption at 490 nm	$astarOMA$	1.45×10^{-3}
OMZ specific absorption at 490 nm	$astarOMZ$	1.13×10^{-3}
Temperature		
Optimum temperature for growth(C)	$Tref(nospA+nospZ)_{p1}$	0.6
Phytoplankton		
mortality coefficient	mA	13.94
edibility vector for Z1	$ediblevector(Z1)$	0.95
maximum growth rate	$umax$	0.85
initial slope of the photosynthesis-irradiance relationship	$alpha$	0.62
N-uptake rate measured at umax	$vmaxN$	0.53
phytoplankton growth respiration coefficient	$respg$	0.26
Phytoplankton threshold for grazing, is multiplied by VOLcell	$Athresh$	0.25
phytoplankton basal respiration coefficient	$respb$	0.24
coefficient for non-limiting nutrient	aN	0.17
half-saturation constant for P	Kp	0.14
P-uptake rate measured at umax	$vmaxP$	0.12
phytoplankton volume/cell	$volcell$	0.1
minimum N cell-quota	$QminN$	0.07
phytoplankton carbon/cell	Qc	0.02
half-saturation constant for N	Kn	0.01
minimum P cell-quota	$QminP$	1.38×10^{-6}
Zooplankton		
maximum growth rate of zooplankton	$Zumax$	1.02
half saturation coefficient for grazing	ZKa	0.85
assimilation efficiency as a fraction of ingestion	$Zeffic$	0.57
zooplankton nitrogen/individual	ZQn	0.52
Zooplankton mortality constant for quadratic mortality	Zm	0.41
proportion of grazed phytoplankton lost to sloppy feeding	$Zslop$	0.23
Zooplankton growth-dependent respiration factor	$Zrespg$	0.17
Zooplankton biomass-dependent respiration factor	$Zrespb$	0.14
zooplankton phosphorus/individual	ZQp	1.29×10^{-3}
zooplankton carbon/individual	ZQc	7.55×10^{-5}
Organic Matter		
decay rate of CDOM, 1/day	$KGcdom$	0.07
turnover rate for OM1A and OM1Z	$KG1$	0.03
turnover rate for OM2A and OM2Z	$KG2$	0.01
O2 concentration that inhibits denitrification	$KstarO2$	0.01
half-saturation concentration for O2 utilization	$KO2$	3.35×10^{-3}
half-saturation concentration for NO3 used in denitrification	$KNO3$	1.19×10^{-3}
maximum rate of nitrification per day	$nitmax$	3.4×10^{-5}
NH4 rate constant for nitrification	$KNH4$	2.97×10^{-5}

Table S3: Sensitivity of irradiance to perturbations of individual parameters. Sensitivities are based on a 50% increase from the initial parameter value, where $L1$ summarizes differences in model output from the default (see eq. (2)). Parameters that did not affect irradiance are not shown. Parameters are grouped by categories as optics, temperature, phytoplankton, zooplankton, and organic matter.

Description	Parameter	L1
Optics		
Chla specific absorption at 490 nm	$astar490$	0.02
OMA specific absorption at 490 nm	$astarOMA$	1.47×10^{-3}
OMZ specific absorption at 490 nm	$astarOMZ$	1.34×10^{-3}
Temperature		
Optimum temperature for growth(C)	$Tref(nospA+nospZ)_{p1}$	0.03
Phytoplankton		
maximum growth rate	$umax$	0.09
mortality coefficient	mA	0.05
initial slope of the photosynthesis-irradiance relationship	$alpha$	0.04
edibility vector for Z1	$ediblevector(Z1)$	0.04
N-uptake rate measured at umax	$vmaxN$	0.03
Phytoplankton threshold for grazing, is multiplied by VOLcell	$Athresh$	0.02
coefficient for non-limiting nutrient	aN	0.01
phytoplankton growth respiration coefficient	$respg$	0.01
half-saturation constant for P	Kp	0.01
P-uptake rate measured at umax	$vmaxP$	9.48×10^{-3}
phytoplankton basal respiration coefficient	$respb$	9.38×10^{-3}
phytoplankton volume/cell	$volcell$	8.1×10^{-3}
minimum N cell-quota	$QminN$	5.75×10^{-3}
phytoplankton carbon/cell	Qc	3.78×10^{-3}
half-saturation constant for N	Kn	9.81×10^{-4}
minimum P cell-quota	$QminP$	1.92×10^{-7}
Zooplankton		
half saturation coefficient for grazing	ZKa	0.13
zooplankton nitrogen/individual	ZQn	0.06
maximum growth rate of zooplankton	$Zumax$	0.04
Zooplankton mortality constant for quadratic mortality	Zm	0.04
assimilation efficiency as a fraction of ingestion	$Zeffic$	0.03
proportion of grazed phytoplankton lost to sloppy feeding	$Zslop$	0.02
Zooplankton growth-dependent respiration factor	$Zrespg$	0.01
Zooplankton biomass-dependent respiration factor	$Zrespb$	9.67×10^{-3}
zooplankton phosphorus/individual	ZQp	9.34×10^{-5}
zooplankton carbon/individual	ZQc	1.99×10^{-5}
Organic Matter		
decay rate of CDOM, 1/day	$KGcdom$	0.05
turnover rate for OM1A and OM1Z	$KG1$	3.96×10^{-3}
turnover rate for OM2A and OM2Z	$KG2$	9.88×10^{-4}
O2 concentration that inhibits denitrification	$KstarO2$	7.2×10^{-4}
half-saturation concentration for O2 utilization	$KO2$	3.54×10^{-4}
half-saturation concentration for NO3 used in denitrification	$KNO3$	6.18×10^{-5}
maximum rate of nitrification per day	$nitmax$	1.72×10^{-6}
NH4 rate constant for nitrification	$KNH4$	1.48×10^{-6}

Table S4: Sensitivity of nitrate to perturbations of individual parameters. Sensitivities are based on a 50% increase from the initial parameter value, where $L1$ summarizes differences in model output from the default (see eq. (2)). Parameters that did not affect nitrate are not shown. Parameters are grouped by categories as optics, temperature, phytoplankton, zooplankton, and organic matter.

Description	Parameter	L1
Optics		
Chla specific absorption at 490 nm	astar490	0.02
OMZ specific absorption at 490 nm	astarOMZ	1.27×10^{-3}
OMA specific absorption at 490 nm	astarOMA	1.19×10^{-3}
Temperature		
Optimum temperature for growth(C)	$Tref(nospA+nospZ)_{p1}$	0.3
Phytoplankton		
maximum growth rate	umax	8.49
phytoplankton carbon/cell	Qc	0.89
initial slope of the photosynthesis-irradiance relationship	alpha	0.7
edibility vector for Z1	ediblevector(Z1)	0.33
mortality coefficient	mA	0.27
Phytoplankton threshold for grazing, is multiplied by VOLcell	Athresh	0.2
N-uptake rate measured at umax	vmaxN	0.19
coefficient for non-limiting nutrient	aN	0.13
phytoplankton growth respiration coefficient	respg	0.11
phytoplankton volume/cell	volcell	0.1
P-uptake rate measured at umax	vmaxP	0.1
half-saturation constant for P	Kp	0.09
minimum N cell-quota	QminN	0.09
phytoplankton basal respiration coefficient	respb	0.07
half-saturation constant for N	Kn	7.06×10^{-3}
minimum P cell-quota	QminP	6.67×10^{-7}
Zooplankton		
half saturation coefficient for grazing	ZKa	7.59
zooplankton nitrogen/individual	ZQn	1.17
Zooplankton mortality constant for quadratic mortality	Zm	0.7
maximum growth rate of zooplankton	Zumax	0.34
proportion of grazed phytoplankton lost to sloppy feeding	Zslop	0.26
assimilation efficiency as a fraction of ingestion	Zeffic	0.25
Zooplankton growth-dependent respiration factor	Zrespg	0.17
Zooplankton biomass-dependent respiration factor	Zrespb	0.1
zooplankton carbon/individual	ZQc	3.8×10^{-3}
zooplankton phosphorus/individual	ZQp	8.59×10^{-4}
Organic Matter		
O2 concentration that inhibits denitrification	KstarO2	0.78
half-saturation concentration for NO3 used in denitrification	KNO3	0.07
decay rate of CDOM, 1/day	KGcdom	0.04
half-saturation concentration for O2 utilization	KO2	0.03
turnover rate for OM1A and OM1Z	KG1	0.02
turnover rate for OM2A and OM2Z	KG2	0.01
maximum rate of nitrification per day	nitmax	9.96×10^{-3}
NH4 rate constant for nitrification	KNH4	9.87×10^{-3}

Table S5: Sensitivity of POM to perturbations of individual parameters. Sensitivities are based on a 50% increase from the initial parameter value, where $L1$ summarizes differences in model output from the default (see eq. (2)). Parameters that did not affect POM are not shown. Parameters are grouped by categories as optics, temperature, phytoplankton, zooplankton, and organic matter.

Description	Parameter	L1
Optics		
Chla specific absorption at 490 nm	*astar490*	0.03
OMA specific absorption at 490 nm	*astarOMA*	1.73×10^{-3}
OMZ specific absorption at 490 nm	*astarOMZ*	1.49×10^{-3}
Temperature		
Optimum temperature for growth(C)	$Tref(nospA+nospZ)_{p1}$	0.86
Phytoplankton		
mortality coefficient	*mA*	7.22
edibility vector for Z1	*ediblevector(Z1)*	0.9
maximum growth rate	*umax*	0.89
phytoplankton carbon/cell	*Qc*	0.67
initial slope of the photosynthesis-irradiance relationship	*alpha*	0.67
N-uptake rate measured at umax	*vmaxN*	0.45
phytoplankton growth respiration coefficient	*respg*	0.29
phytoplankton basal respiration coefficient	*respb*	0.24
Phytoplankton threshold for grazing, is multiplied by VOLcell	*Athresh*	0.22
minimum N cell-quota	*QminN*	0.21
coefficient for non-limiting nutrient	*aN*	0.14
half-saturation constant for P	*Kp*	0.11
phytoplankton volume/cell	*volcell*	0.1
P-uptake rate measured at umax	*vmaxP*	0.09
half-saturation constant for N	*Kn*	0.01
minimum P cell-quota	*QminP*	7.35×10^{-4}
Zooplankton		
maximum growth rate of zooplankton	*Zumax*	0.96
half saturation coefficient for grazing	*ZKa*	0.79
assimilation efficiency as a fraction of ingestion	*Zeffic*	0.54
zooplankton nitrogen/individual	*ZQn*	0.49
Zooplankton mortality constant for quadratic mortality	*Zm*	0.39
proportion of grazed phytoplankton lost to sloppy feeding	*Zslop*	0.27
Zooplankton growth-dependent respiration factor	*Zrespg*	0.16
Zooplankton biomass-dependent respiration factor	*Zrespb*	0.12
zooplankton carbon/individual	*ZQc*	9.64×10^{-3}
zooplankton phosphorus/individual	*ZQp*	1.06×10^{-3}
Organic Matter		
turnover rate for OM1A and OM1Z	*KG1*	0.92
decay rate of CDOM, 1/day	*KGcdom*	0.07
half-saturation concentration for O2 utilization	*KO2*	0.04
O2 concentration that inhibits denitrification	*KstarO2*	0.02
turnover rate for OM2A and OM2Z	*KG2*	0.01
half-saturation concentration for NO3 used in denitrification	*KNO3*	3.72×10^{-3}
maximum rate of nitrification per day	*nitmax*	6.98×10^{-5}
NH4 rate constant for nitrification	*KNH4*	6.41×10^{-5}

Table S6: Sensitivity of dissolved organic matter to perturbations of individual parameters. Sensitivities are based on a 50% increase from the initial parameter value, where $L1$ summarizes differences in model output from the default (see eq. (2)). Parameters that did not affect dissolved organic matter are not shown. Parameters are grouped by categories as optics, temperature, phytoplankton, zooplankton, and organic matter.

Description	Parameter	L1
Optics		
Chla specific absorption at 490 nm	$astar490$	0.04
OMA specific absorption at 490 nm	$astarOMA$	2.48×10^{-3}
OMZ specific absorption at 490 nm	$astarOMZ$	2.04×10^{-3}
Temperature		
Optimum temperature for growth(C)	$Tref(nospA+nospZ)_{p1}$	1.48
Phytoplankton		
mortality coefficient	mA	14.25
maximum growth rate	$umax$	1.11
edibility vector for Z1	$ediblevector(Z1)$	0.94
N-uptake rate measured at umax	$vmaxN$	0.86
initial slope of the photosynthesis-irradiance relationship	$alpha$	0.85
phytoplankton carbon/cell	Qc	0.67
phytoplankton growth respiration coefficient	$respg$	0.36
phytoplankton basal respiration coefficient	$respb$	0.29
coefficient for non-limiting nutrient	aN	0.25
minimum N cell-quota	$QminN$	0.24
Phytoplankton threshold for grazing, is multiplied by VOLcell	$Athresh$	0.22
half-saturation constant for P	Kp	0.2
P-uptake rate measured at umax	$vmaxP$	0.14
phytoplankton volume/cell	$volcell$	0.1
half-saturation constant for N	Kn	0.02
minimum P cell-quota	$QminP$	4.37×10^{-3}
Zooplankton		
maximum growth rate of zooplankton	$Zumax$	1.01
half saturation coefficient for grazing	ZKa	0.88
assimilation efficiency as a fraction of ingestion	$Zeffic$	0.58
zooplankton nitrogen/individual	ZQn	0.54
Zooplankton mortality constant for quadratic mortality	Zm	0.41
Zooplankton growth-dependent respiration factor	$Zrespg$	0.17
Zooplankton biomass-dependent respiration factor	$Zrespb$	0.13
proportion of grazed phytoplankton lost to sloppy feeding	$Zslop$	0.12
zooplankton carbon/individual	ZQc	0.04
zooplankton phosphorus/individual	ZQp	1.69×10^{-3}
Organic Matter		
turnover rate for OM2A and OM2Z	$KG2$	0.94
decay rate of CDOM, 1/day	$KGcdom$	0.1
half-saturation concentration for O2 utilization	$KO2$	0.04
turnover rate for OM1A and OM1Z	$KG1$	0.04
O2 concentration that inhibits denitrification	$KstarO2$	0.03
half-saturation concentration for NO3 used in denitrification	$KNO3$	3.16×10^{-3}
maximum rate of nitrification per day	$nitmax$	8.44×10^{-5}
NH4 rate constant for nitrification	$KNH4$	7.41×10^{-5}

Table S7: Sensitivity of phosphate to perturbations of individual parameters. Sensitivities are based on a 50% increase from the initial parameter value, where $L1$ summarizes differences in model output from the default (see eq. (2)). Parameters that did not affect phosphate are not shown. Parameters are grouped by categories as optics, temperature, phytoplankton, zooplankton, and organic matter.

Description	Parameter	L1
Optics		
Chla specific absorption at 490 nm	$astar490$	9.01×10^{-3}
OMZ specific absorption at 490 nm	$astarOMZ$	5.21×10^{-4}
OMA specific absorption at 490 nm	$astarOMA$	5.13×10^{-4}
Temperature		
Optimum temperature for growth(C)	$Tref(nospA+nospZ)_{p1}$	0.16
Phytoplankton		
maximum growth rate	$umax$	0.78
P-uptake rate measured at umax	$vmaxP$	0.59
edibility vector for Z1	$ediblevector(Z1)$	0.25
initial slope of the photosynthesis-irradiance relationship	$alpha$	0.23
mortality coefficient	mA	0.2
N-uptake rate measured at umax	$vmaxN$	0.18
Phytoplankton threshold for grazing, is multiplied by VOLcell	$Athresh$	0.13
coefficient for non-limiting nutrient	aN	0.11
phytoplankton growth respiration coefficient	$respg$	0.09
phytoplankton volume/cell	$volcell$	0.06
phytoplankton basal respiration coefficient	$respb$	0.06
minimum N cell-quota	$QminN$	0.04
half-saturation constant for P	Kp	0.03
half-saturation constant for N	Kn	6.97×10^{-3}
phytoplankton carbon/cell	Qc	6.68×10^{-3}
minimum P cell-quota	$QminP$	8.21×10^{-7}
Zooplankton		
half saturation coefficient for grazing	ZKa	1.47
zooplankton nitrogen/individual	ZQn	0.5
Zooplankton mortality constant for quadratic mortality	Zm	0.35
maximum growth rate of zooplankton	$Zumax$	0.26
assimilation efficiency as a fraction of ingestion	$Zeffic$	0.19
proportion of grazed phytoplankton lost to sloppy feeding	$Zslop$	0.15
Zooplankton growth-dependent respiration factor	$Zrespg$	0.1
Zooplankton biomass-dependent respiration factor	$Zrespb$	0.06
zooplankton phosphorus/individual	ZQp	6.43×10^{-3}
zooplankton carbon/individual	ZQc	3.38×10^{-5}
Organic Matter		
turnover rate for OM1A and OM1Z	$KG1$	0.14
turnover rate for OM2A and OM2Z	$KG2$	0.06
decay rate of CDOM, 1/day	$KGcdom$	0.02
half-saturation concentration for O2 utilization	$KO2$	0.01
O2 concentration that inhibits denitrification	$KstarO2$	7.29×10^{-3}
half-saturation concentration for NO3 used in denitrification	$KNO3$	1.19×10^{-3}
maximum rate of nitrification per day	$nitmax$	2.7×10^{-5}
NH4 rate constant for nitrification	$KNH4$	2.64×10^{-5}